

**Appendix G: Benchmark Analysis with JASMINE and
CFAST, Stewart MILES, BRE, UK**

International Collaborative Project to Evaluate Fire Models for Nuclear Power
Plant Applications

Benchmark Exercise # 1 - Cable Tray Fires of Redundant Safety Trains

Simulations using JASMINE and CFAST

S.D. Miles

Building Research Establishment, UK

SUMMARY

As part of its participation in the International Collaborative Project to Evaluate Fire Models for Nuclear Power Plant Applications, BRE has made numerical predictions for Benchmark Exercise # 1 – cable tray fires of redundant safety trains. Trash bag and cable tray fires inside a switchgear room were modelled, with the main objective to ascertain the likelihood of thermal damage to a 'target' cable at various distances from the fire source.

BRE has performed simulations using a CFD model (JASMINE) and a zone model (CFAST). Results and analysis were presented at a meeting of the collaborative project in January 2001. This paper summarises the findings from the BRE simulations.

Due to the nature of the benchmark scenarios, both CFAST and JASMINE indicated that damage to the target cables was unlikely in all scenarios. However, some important observations were made, including the difficulty in modelling nearly-sealed rooms where the difference in pressure predicted by CFAST and JASMINE providing the most noticeable difference in the output from the two models. Other issues that were found to be important included the modelling/assessment of the heating of the target cables, and the influence of using different oxygen starvation criteria and fire source locations.

INTRODUCTION

In October 1999 the U.S. Nuclear Regulatory Commission and the Society of Fire Protection Engineers organised a planning meeting with international experts and practitioners of fire models to discuss the evaluation of numerical fire models for nuclear power plant applications. Following this meeting an international collaborative project was set up with a view to sharing knowledge and resources from various organisations and to evaluate and improve the state of the fire modelling methods and tools for use in nuclear power plant fire safety.

The UK Building Research Establishment (BRE) was represented at the next meeting of the collaborative project (ISPN, Paris, June 2000). The main outcome from this meeting was a finalised problem definition for a nuclear power plant fire scenario, to be used as a benchmark exercise for which the participating organisations would undertake numerical predictions and then compare results.

BRE's Fire and Risk Sciences (FRS) Division performed zone model (CFAST) and CFD (JASMINE) simulations of selected scenario cases from the benchmark exercise. Results and analysis were presented during the third meeting of the international collaborative project at the Electric Power Research Institute (EPRI), California in January 2001.

This paper summarises the CFAST and JASMINE simulations and findings. Following sections describing briefly the fire models used, there is a section highlighting the main results and analyses.

CFAST DESCRIPTION

CFAST is one of the most widely used zone models, available from the National Institute of Standards and Technology (NIST), USA. It is the main component of the program suite FAST, which is controlled through a graphical user interface. CFAST/FAST version 3.1.6 was used in the current study, which is the most recent complete version to be released.

CFAST is a multi-room zone model, with the capability to model multiple fires and targets. Fuel pyrolysis rate is a pre-defined input, and the burning in the compartment is then modelled to generate heat release and allow species concentrations to be calculated. For most applications CFAST is used as a conventional two-zone model, whereby each compartment is divided into a hot gas upper layer and a cold lower layer. In the presence of fire, a plume zone/model transports heat and mass from the lower to upper layer making use of the McCaffrey correlation [1]. Flows through vents and doorways are determined from correlations derived from the Bernoulli equation. Radiation heat transfer may be included using an algorithm derived from that of Siegel and Howell [2]. Other features of CFAST of relevance to the benchmark exercise include a one-dimensional solid phase heat conduction algorithm employed at compartment walls and targets and network flow model for mechanical ventilation.

Publications available on the NIST website (www.nist.gov) [3,4] provide a comprehensive description of CFAST and the models employed. A summary of comparison with experimental measurements is provided also.

JASMINE DESCRIPTION

JASMINE is a CFD fire code that has undergone continual development at the BRE over nearly 20 years. It simulates fire and smoke movement in three-dimensions, for steady state and time-dependent applications. Version JASMINE 3.1 was used in this benchmark exercise.

JASMINE is a finite-volume CFD code, employing a variant of the SIMPLE pressure-correction scheme on a structured, Cartesian mesh. The program can model single and multiple compartment enclosures with arbitrary openings (doors, windows and vents), obstructions, fire/heat sources and mechanical ventilation systems. External wind profiles, static pressure boundaries and symmetry planes may be specified.

A modified, enhanced version of an early PHOENICS code provides the core pressure-correction solver. Turbulent closure is by a $k-\epsilon$ model using the standard constants and additional buoyancy source terms. Standard wall functions for enthalpy and momentum describe the turbulent boundary layer adjacent to solid surfaces. A suite of sub-models for combustion, radiation, data analysis etc has been added as part of the code development.

A scenario may be set-up using the graphical user interface (JOSEFINE), which allows the user to define the geometry and boundary conditions and view the results with a graphical post-processor. The results may be viewed also with the commercial CFD post processor FIELDVIEW. A detailed summary text file is generated, containing convergence information, analysis data etc.

JASMINE has been validated against data from pre-flashover fire experiments inside domestic size rooms, atria, tunnels, hospital wards and other enclosures. More recently it has been validated against data from post-flashover fire tests also. Further details are provided in the validation section.

Modelling Details

Mathematical details of the differential-integral equations describing the fluid flow processes may be found elsewhere, see for example [5]. In summary, the equations describing the fluid dynamics of Newtonian fluids (which includes most common fluids such as air and water) are the Navier-Stokes equations for momentum and mass conservation and the related advection-diffusion transport equation describing conservation of other properties such as energy and species concentration. These equations, together with equations of state for density and temperature, describe very accurately the physics of Newtonian fluids.

CFD models approximate the underlying equations with a coupled system of algebraic equations that are solved numerically on a discrete mesh or grid. This yields predictions for velocity, pressure, temperature etc at each mesh point in space and time. JASMINE, in common with most other CFD fire models, employs the finite volume method [6,7], in which the differential equations are first transformed into an integral form and then discretised on the control volumes defined by the mesh.

JASMINE solves a time/ensemble-averaged form of the Navier-Stokes and transport equations, where the turbulent fluctuations are not modelled explicitly, but instead are 'incorporated' into the solution by a 'turbulence model'. The particular model used in JASMINE is the industry standard, $k-\epsilon$ model [8], which employs the eddy viscosity assumption in which the effect of turbulence is included as an additional 'turbulent viscosity'. Additional source terms are included in the $k-\epsilon$ model to account for the effects of buoyancy [9].

The ensemble-averaged Navier-Stokes and transport equations, coupled with an equation of state (ideal gas law) and the various sub-models for the fire physics, defines the equation set in JASMINE. This is discretised and solved numerically on a structured three-dimensional grid using the SIMPLEST scheme, a variant of the SIMPLE pressure-correction scheme [7,10]. Convection terms are discretised with the first-order 'upwind' scheme and time advancement is by the first-order, fully implicit, backward Euler scheme. Standard wall functions for enthalpy and momentum [8] describe the turbulent boundary layer adjacent to solid surfaces.

Combustion is generally modelled using an eddy breakup assumption [11] in which the fuel pyrolysis rate is specified as a boundary condition, and combustion is then calculated at all control volumes as a function of fuel concentration, oxygen concentration and the local turbulent time-scale (provided by the $k-\epsilon$ model). Simple one-step, infinitely fast chemical reaction is assumed. The eddy breakup model is appropriate for turbulent diffusion flames characteristic of fire, where the rate of reaction is controlled by the comparatively slow mixing of fuel with oxygen. Complete oxidation of the fuel is assumed when sufficient oxygen is available, and therefore predictions of carbon monoxide are not provided by this approach.

Radiant heat transfer is modelled with either the six-flux model [12], which assumes that radiant transfer is normal to the co-ordinate directions or the slower, but potentially more accurate, discrete transfer method [13]. Local absorption-emission properties are computed using Truelove's mixed grey-gas model [14], which calculates the local absorption coefficient as a function of temperature and gas species concentrations and, if available, soot concentration also.

Density is defined from the equation of state, and gas temperature is calculated from the definition of enthalpy, in which specific heat is itself a function of temperature and species concentrations. Thermal conduction into solid boundaries is approximated by a quasi-steady, semi-infinite one-dimensional assumption.

Code Validation

JASMINE has been validated against experimental measurement for a range of scenarios, ranging from small enclosure fire experiments to large, fully developed fires in tunnels and offshore structures. Some of the more important validation cases are referenced below.

The Steckler experiments [15]. In these experiments steady state mass flow rates, velocity profiles and temperatures associated with a burner at various locations inside a 2.8 m x 2.8 m x 2.18 m compartment with a single doorway opening were measured. Good agreement was found for the doorway flow rates, with the CFD model capturing the influence of plume lean on the entrainment process.

The Lawrence Livermore experiments [16]. A series of steady state experiments were performed with a spray pool fire inside a 6 m x 4 m x 4.5 m nuclear test cell with mechanical ventilation. Good agreement was obtained for temperatures inside the test cell, and the prediction of fire-induced pressure rise was reasonably close to the measured value.

Hospital ward experiments [17]. An experiment was performed involving a burning PU-foam mattress in a ward of dimensions 7.3 m x 7.9 m x 2.7 m. Pre-fire steady condition, driven by the heat released from a set of wall radiators, and the subsequent transient fire phase were simulated. Good temperature agreement was achieved, and good species (CO_2) agreement at head height also. However, there was some discrepancy in CO_2 at bedside height.

Sports stadium [18]. Simulations were made of fire tests performed in a 1/6th-scale physical model of a proposed sports stadium. Comparisons were made for temperatures at thermocouple tree locations, which showed good agreement. Some discrepancy at ceiling level was attributed to the approximate 'staircase' representation of the dome shape.

Zwenberg railway tunnel experiments [19,20]. Predictions made by TUNFIRE, the tunnel specific version of JASMINE, were compared to measurements from a series of fire tests in the disused Zwenberg railway tunnel in Austria. The tunnel is 390 m long with a 2.18% gradient. Steady state scenarios involving natural and forced longitudinal ventilation with fires of approximately 20 MW were modelled. Predictions of the temperature and species downstream of the fire source were in good agreement with measurement. However, the need for further model development in the treatment of radiation and heat transfer in the vicinity of the fire was highlighted.

Memorial Tunnel experiments [21]. The decommissioned Memorial Tunnel in the USA was used for an extensive set of fire tests involving natural, longitudinal and transverse ventilation. A selection of the longitudinal ventilation tests, involving pool fires from 20 to 100 MW, was modelled with TUNFIRE. The transient simulations captured the main features of the tests, predicating the performance of various jet fan configurations reasonably well. Some discrepancy was found in the pre-ventilation stage where the smoke layer dropped to ground level more quickly in the simulations compared to the tests.

Channel Tunnel shuttle wagon tests [22]. As part of the safety study for the Channel Tunnel, JASMINE was validated against fire experiments inside a car shuttle wagon. It was shown that by considering properly the mechanical ventilation system and the boundary heat losses reasonably good agreement could be achieved for temperature and gas species.

LBTf tests [23]. An eight-storey, steel framed building, constructed at BRE's Cardington Hanger, provided an ideal opportunity to perform full-scale fire tests. The 8.4 m high atrium and part of the first floor were used in the study of fully-ventilated fires up to 5 MW in size. Predictions of smoke layer depth and temperature matched experimental measurement reasonably closely, as did the entrainment rates.

Post-flashover compartment fire tests [24]. A series of fully developed, ventilation-controlled fire tests was sponsored by the European offshore industry to validate zone and CFD models. Tests involving pool fires up to 80 MW inside single opening enclosures were modelled with JASMINE. Good agreement was found in the vent flow rates and temperatures. Furthermore, the simulations captured the oxygen depletion process correctly. The main discrepancy was in the temperatures and fluxes at the back of the compartment, attributed in part to the

complexity of the wall lining behaviour, which involved the steel sheeting becoming partly detached during the tests.

CIB round robin activity [25]. The Commission of the International Council for Research and Innovation in Building and Construction (CIB) co-ordinated a series of round robin fire model validation exercises in which participants made 'blind' predictions for fire tests in the knowledge of only a limited amount of information (geometry, thermal properties, fire pyrolysis rate). JASMINE simulations were made for a compartment (7.2 m x 7.2 m x 3.6 m) with a 'letter-box' opening and two crib fire sources. Good agreement was found for species predictions, and reasonable agreement for temperatures. Predicted incident wall fluxes were noticeably lower than those 'estimated' from the measurement data, attributed in part to the quasi-steady heat conduction treatment used in the simulations.

Balcony spill plume tests [26]. As part of a wider study into the entrainment processes associated with spill plumes, JASMINE simulations of various 1/10th-scale experiments were performed. Predicted and measured entrainment rates were in reasonable agreement. An important conclusion was that grid refinement did have an important influence on the predicted entrainment rate.

Sprinkler model validation [27]. As part of the development of a sprinkler model for JASMINE, simulations were undertaken of a full-scale fire test where the influence of the water spray on gas temperatures and velocities at ceiling level was investigated. Reasonable agreement was found, and areas of further improvement identified.

BENCHMARK EXERCISE

Problem Definition

Following publication of the specification for the benchmark exercise # 1, BRE has undertaken CFD (JASMINE) and zone model (CFAST) predictions for selected scenario cases. The benchmark exercise is described in Appendix A.

Table 1 shows the scenario cases modelled by BRE. Due to the long duration of the Part II scenarios (80 minutes), the CFD (JASMINE) simulations were undertaken for between 20 and 45 minutes only (depending on the case). This was sufficiently long to investigate the main features of each scenario, and allowed more cases to be undertaken with the available computing resource. Whereas individual JASMINE simulations were undertaken for each Part I case, some of the Part II cases were 'doubled up' in that a CFD solution was used to investigate more than one case. This was due to some cases differing only in the location of the target cable, which itself did not influence the CFD solution, i.e. one CFD solution was used to predict the thermal damage to multiple target locations.

Table 1. Benchmark scenarios modelled

Numerical Model	Scenarios Modelled
JASMINE	Part I: base case, case 1 and case 4 Part II: base case and cases 1,2, 9,10,11,12 & 13
CFAST	Part I: all cases Part II: all cases

While the problem specification was followed as closely as possible, some user interpretation was required, in particular in respect to the target description and the treatment of radiation. Most simulations were completed prior to the third project meeting, and the findings were presented at that meeting. Some further simulations have been performed since, looking at the effect of mechanical ventilation with CFAST and the prediction of pressure in the door-crack scenarios with JASMINE.

In CFAST, heat transfer to a rectangular target object, orientated in a particular direction, can be modelled using a one-dimensional equation. The simulations showed that the choice of target orientation could have a significant influence on the size of the incident heat flux. JASMINE also allows heat transfer to solid objects to be modelled using a semi-infinite, quasi-steady approximation. For the current work, however, an assessment of the likelihood of target cable damage was based on the local gas temperature and mean radiation flux. This will in general provide a conservative approach, over-predicting the thermal hazard.

For the CFAST simulations radiation from the fire plume was incorporated, as specified, by reducing the fire size by 30%. For the JASMINE simulations a six-flux radiation model was employed, and rather than defining the radiation loss explicitly it was predicted by the solution of the CFD and radiation models. Some later simulations investigated the effect of using a fixed radiation loss of 30% and no radiation model.

The two-zone assumption was used for all the CFAST simulations. A constrained fire was assumed, which allowed for oxygen availability to control the rate of heat release from the pre-defined pyrolysed fuel. As stipulated in the benchmark specification, a 30% radiative loss was included. Although the wall and ceiling thermal properties were specified exactly, the separate door properties were not included. To investigate the effect of orientation on the predictions of target surface temperature, two normal directions were considered, namely facing towards the ceiling and towards the floor. The ceiling jet sub-model was used.

The JASMINE simulations employed between 124,000 and 175,000 control volumes, resolving the vertical extent of the door crack with two control volumes. An eddy break-up combustion model was used, which allowed the oxidation of the pre-defined pyrolysed fuel to be calculated as a function of oxygen concentration and local turbulent mixing. The six-flux radiation model, combined with Truelove's emissive power model, was used in the majority of simulations, allowing the radiation losses from the plume and hot gas layer to be calculated with reasonable accuracy. However, to compute fluxes to target cables with greater accuracy would have required the computationally more expensive discrete transfer model. Soot formation and oxidation was not modelled. Although not generally employed in the JASMINE combustion model, a oxygen cut-off was applied in the majority of simulations, using a figure of 12% as requested.

Both JASMINE and CFAST showed that for Part I sufficient oxygen was available for continual combustion in all cases, i.e. the open doorway and door crack cases. The 12% LOL was not reached in either set of simulations. Both models indicated that target cable damage would be very unlikely due to only a modest rise in gas temperature. Figures 1 and 2 show CFAST and JASMINE temperature predictions for the base case and cases 4 and 5 of Part I. Whereas the CFAST values are for the upper layer in the two-zone approximation, the JASMINE temperatures are for a location just below the centre of the ceiling. This will account in part for the difference in predicted values for CFAST and JASMINE, since the CFD model does not consider an average layer/zone temperature. A further point to note is that JASMINE predicted a slight increase in temperature in the presence of mechanical ventilation, which was not shown in the CFAST simulations. Additional, forced airflow will effect the flow pattern in the plume and upper layer, and this is not captured by a zone model. Figure 3 illustrates the effect that mechanical ventilation has on the plume shape in the JASMINE simulations.

A significant finding from the CFAST simulations was that the target orientation could have an important bearing on the incident flux, and resultant target temperature. By facing the target downwards the incident flux was in some instances more than double that obtained when the target faced upwards, as illustrated in Figures 4 and 5. If the target had been directed directly towards the fire, i.e. at an oblique angle, then the incident flux and heating of the cable would most probably been higher still.

Figure 6 shows target radiation fluxes estimated from the JASMINE simulations, where because the target was not modelled explicitly, an average directional flux has been taken. Whereas for case 1 the flux levels are comparable between CFAST and JASMINE, for the other cases examined with JASMINE the similarity is much less. A significant factor here is

that JASMINE models radiation emission and absorption from the gas layer (CO_2 and H_2O), which may be an important transfer mechanism.

As shown in Figures 7-9, both models produced similar flow rates across the doorway for the open doorway scenario (case 4). This scenario represents the classic enclosure fire for which both zone and CFD models would be expected to give similar results.

The most significant difference between the JASMINE and CFAST predictions for Part I was in the pressure predictions for the door crack cases, with CFAST predicting significantly higher pressure build up inside the room. Furthermore, whereas JASMINE predicted outflow from the door crack throughout the duration of the scenario (10 minutes), CFAST predicted a period of moderate inflow after the initial pressure build-up had been dissipated due to venting of gases through the door crack. Figures 10 and 11 show the pressure predictions for CFAST and JASMINE, without (base case) and with (case 5) additional mechanical ventilation. The outflow and subsequent inflow predicted in the CFAST simulation can be seen in Figures 9 and 10.

On initial examination, the pressures predicted by CFAST for the door crack cases (peak value approximately 2000 Pa) seem perhaps too high, whereas the JASMINE values (of the order 50 Pa) seem more reasonable for a compartment fire scenario. While the 'background' pressure level within a sealed compartment is generally not important from the point of modelling fire development (although structural/mechanical considerations may be important), it may be more significant when venting through small orifices is included. Here, the difference in pressure between the inside and outside will have a strong bearing on the flow rate through the opening.

JASMINE adopts the usual assumption adopted in 'low speed' CFD models and treats the air as weakly compressible, i.e. density is defined as a function of temperature and species concentration. The coupling between pressure and density, included in 'high speed' fully compressible models, is ignored. Whether this is important for 'nearly sealed' compartment fire simulations is not clear. CFAST does not solve for conservation of momentum, and the bearing this may have on the door crack scenarios is also not clear.

Further JASMINE analysis of the door crack scenario for Part I has been undertaken since the third meeting of the collaborative project. By defining a 30% radiation loss explicitly, and switching off the radiation model, the period of over-pressure inside the room was followed by a period of under-pressure and associated inflow of outside air. This behaviour was predicted by CFAST, albeit with significantly higher over-pressure. Interestingly, using a volume heat source instead of a combustion model resulted in a higher over-pressure (approximately 120 Pa peak), and again a subsequent period of under-pressure and air inflow. The effect of replacing the door crack with a square opening of equivalent area was investigated, producing a similar result but, as expected, a reduced level of over-pressure. Figure 12 shows the JASMINE pressures for the original base case and also the above modified scenarios. Figure 13 shows that a period of inflow follows, as expected, if the pressure inside the room decreases below ambient.

Clearly the thermodynamics of fire within a 'nearly sealed' compartment is a complex issue that has received much less attention by the fire safety community than fire inside enclosures with at least a moderate level of venting to the outside. Further work in this area is recommended.

For Part II, both JASMINE and CFAST indicated again that target cable damage was unlikely. Oxygen depletion was a significant feature in the door crack cases for Part II, with both models predicting oxygen consumption after about ten minutes. Figure 14 shows the upper layer temperatures predicted by CFAST for the base case and cases 3 and 6 with the larger fires. Figure 15 shows the JASMINE gas temperatures at the target locations for the door-crack scenarios with the smaller fire. The peak temperature at the target location for the base case is similar to the peak upper layer temperature predicted by CFAST. The actual LOL value was not very significant, with the effect of reducing the LOL to zero being to allow combustion to continue for a while longer before stopping due to a lack of available oxygen.

The effect of placing the burning cable tray at floor level was investigated with CFAST, and this did have an influence on the level thermal hazard predicted. In particular, with the larger (3 MW) fire the effect of more combustion occurring before the layer height reached the level of the fire source was an increased upper layer temperature. Figure 16 shows that, combined with a 0% LOL value, this resulted in predicted target surface temperatures that might signify damage. Note that the difference in peak temperature for the three cases is most likely a numerical effect of the model.

However, for both CFAST and JASMINE, a more sophisticated treatment of heat transfer to the target cable, and the subsequent conduction of heat into the cable, would be required in order to obtain more precise estimates of cable temperature and thermal damage. It is likely that the main contributing factor to cable damage for the scenarios like those of Part II would be due to radiative heat transfer from the flaming region, which in cases where the fire source is close to the target cable could be sufficient to cause thermal damage. However, as posed, the Part II scenarios did not allow for this process to be addressed realistically. This was due to the burning area of the fire source being approximated as the entire length of the source (burning) cable, which obviously reduces drastically the intensity of the fire source during the fire growth phase.

In respect to the target orientation issue in CFAST, it was found for Part II that upward facing targets were exposed to greater thermal fluxes than downward facing ones. This was in contrast to Part I, and indicated the importance of this aspect of user interpretation in setting up a scenario.

For Part II, the main discrepancy between CFD and zone model predictions was again in the level of over-pressure in the door crack cases. However, the discrepancy was less than in Part I. Figures 17 and 18 show that the peak over-pressure in the base case was approximately 300 Pa with JASMINE and 750 Pa with CFAST. Furthermore, the CFAST pressure predictions for the door crack cases in Part II were not entirely convincing. As illustrated in Figure 19, placing the cable tray fire source in the base case at floor level resulted in the peak over-pressure increasing from 750 Pa to nearly 5000 Pa, which seems out of proportion compared to the much more modest increase in temperature. Moreover, the peak pressure in excess of 12000 Pa obtained when locating the 3 MW cable tray fire at floor level is certainly surprisingly high.

Cases 9 and 10 of Part II, involving combinations of mechanical ventilation and open doorway conditions, were undertaken with JASMINE. However, in Part II it was not possible to obtain sensible CFAST results with mechanical ventilation.

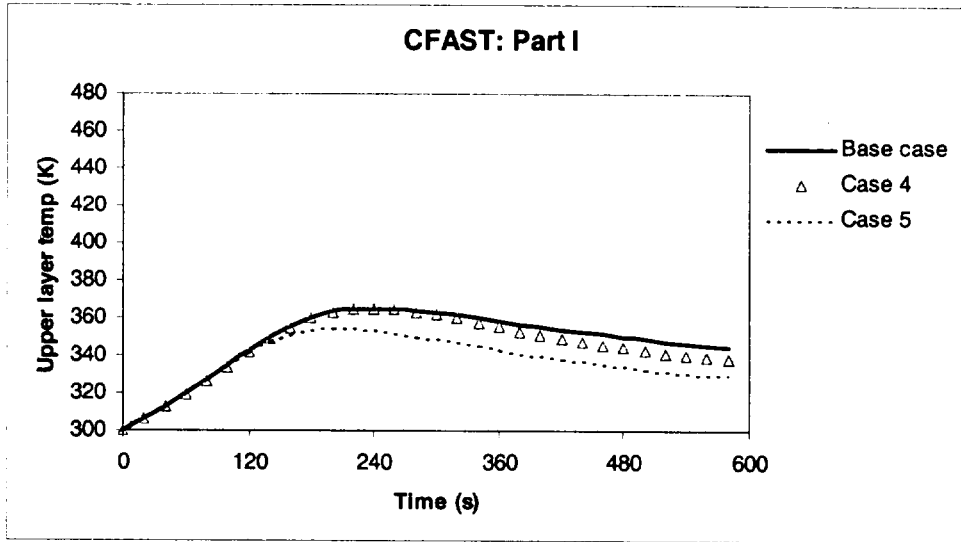


Figure 1 CFAST predictions of upper layer temperatures in Part I

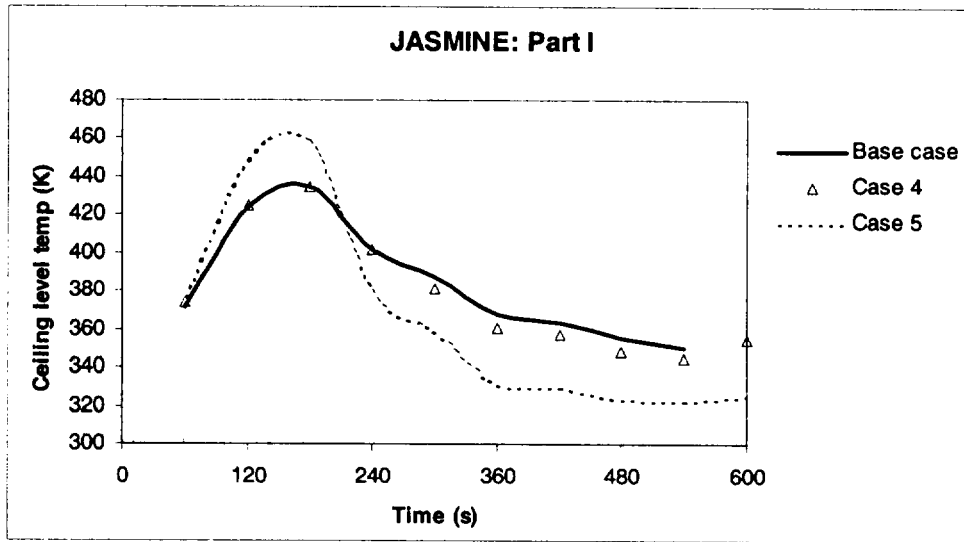
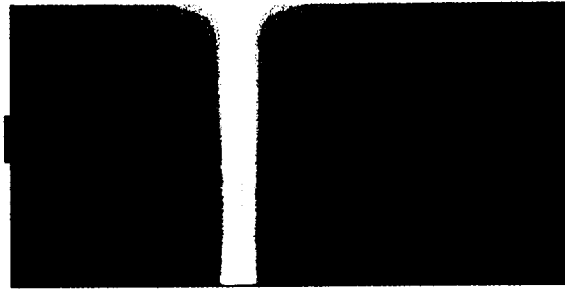
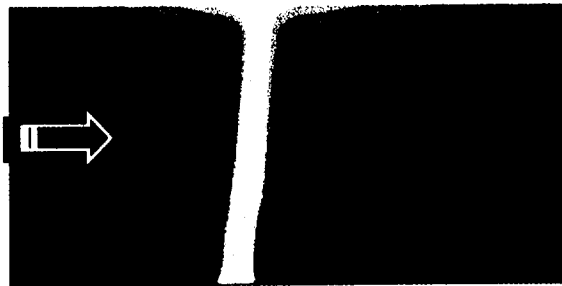


Figure 2 JASMINE predictions of ceiling level temperatures in Part I



Part I base case -- no mechanical ventilation



Part I case 5 - with mechanical ventilation

Figure 3 JASMINE plume shape at 180 s with and without mechanical ventilation

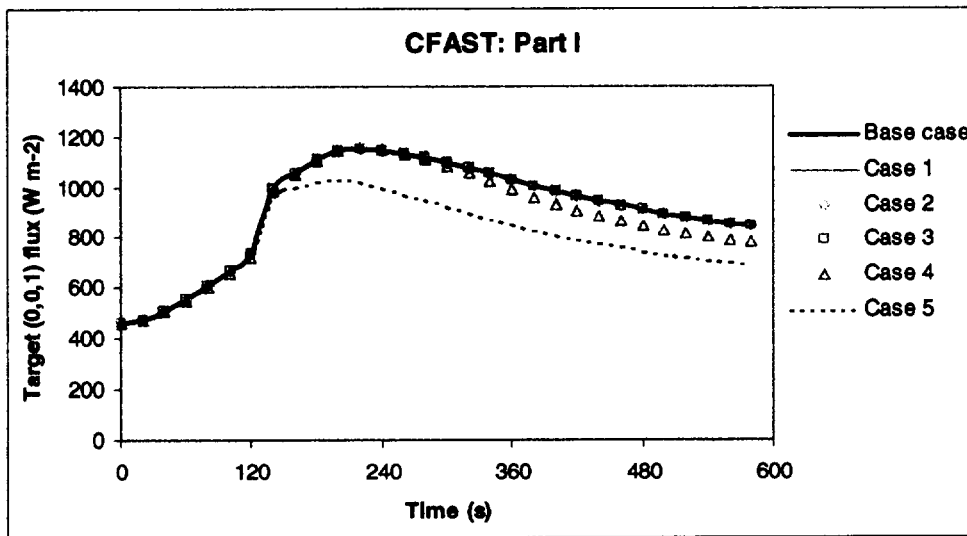


Figure 4 CFAST predictions of fluxes to upward facing targets in Part I

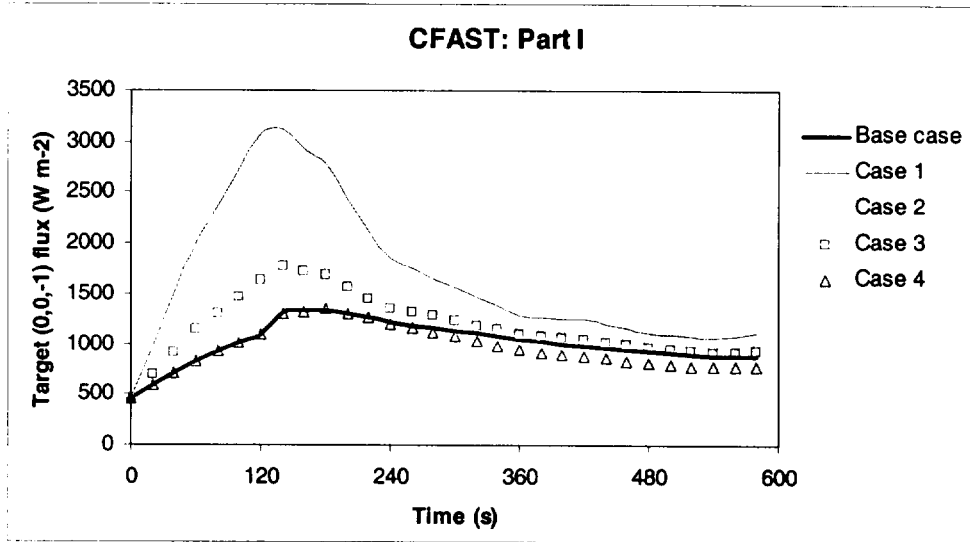


Figure 5 CFAST predictions of fluxes to downward facing targets in Part I

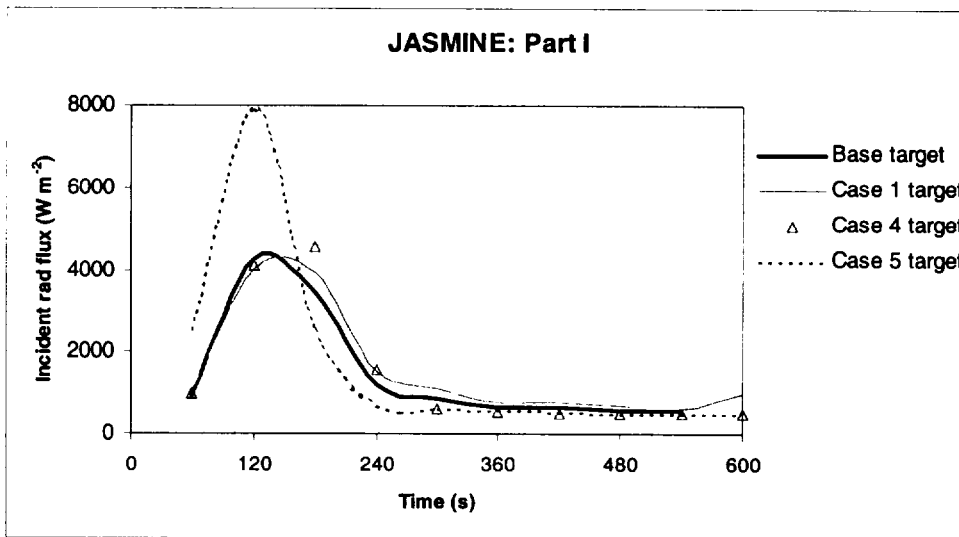


Figure 6 JASMINE predictions of incident fluxes in Part I

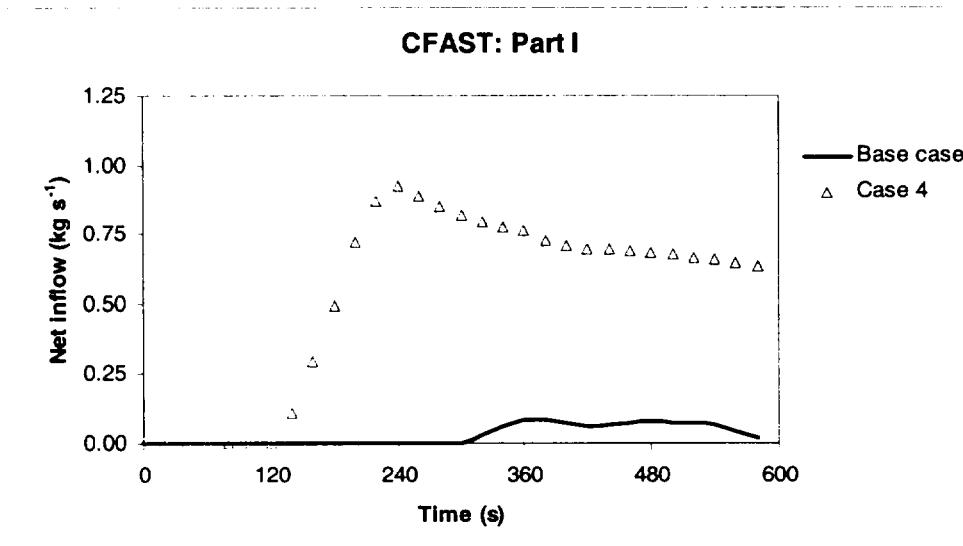


Figure 7 CFAST predictions of inflow rates in Part I

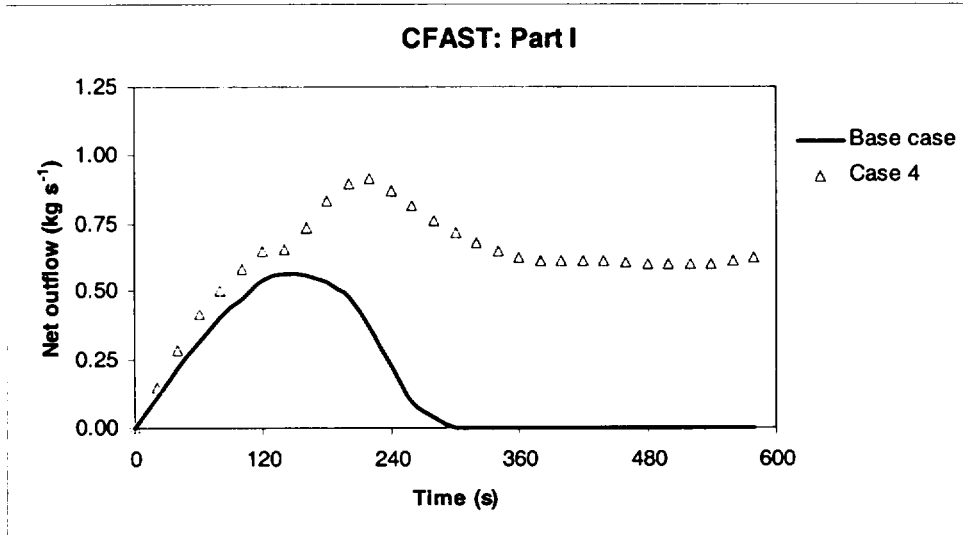


Figure 8 CFAST predictions of outflow rates in Part I

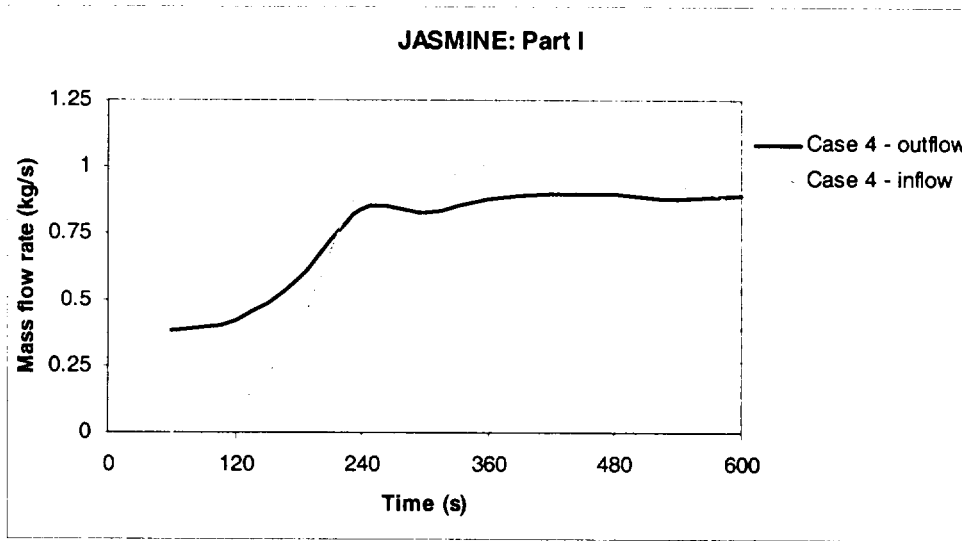


Figure 9 JASMINE predictions of inflow/outflow rates in Part I

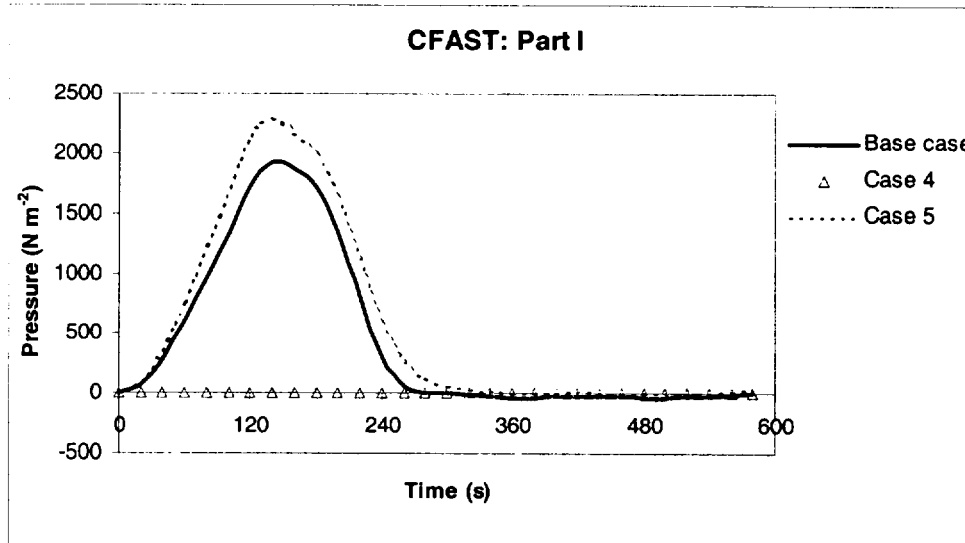


Figure 10 CFAST predictions of pressure in Part I

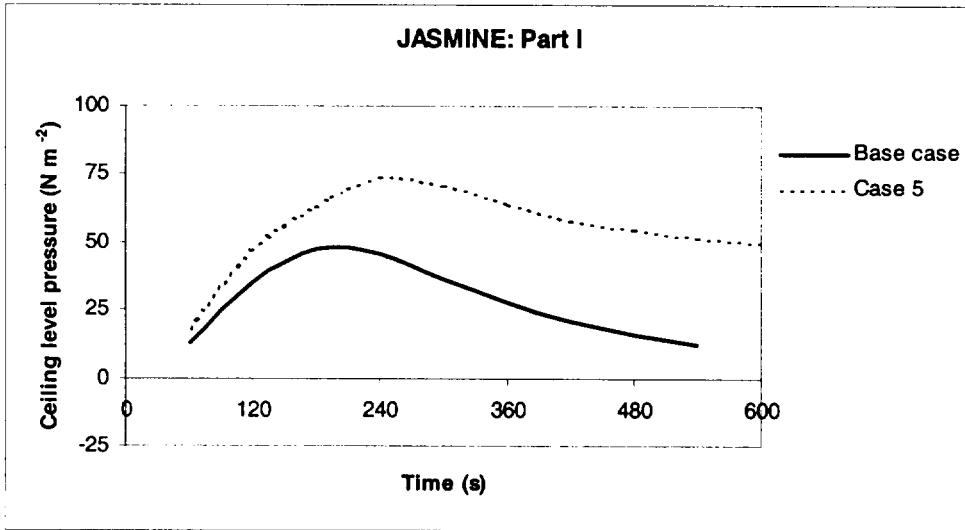


Figure 11 JASMINE predictions of pressure in Part I

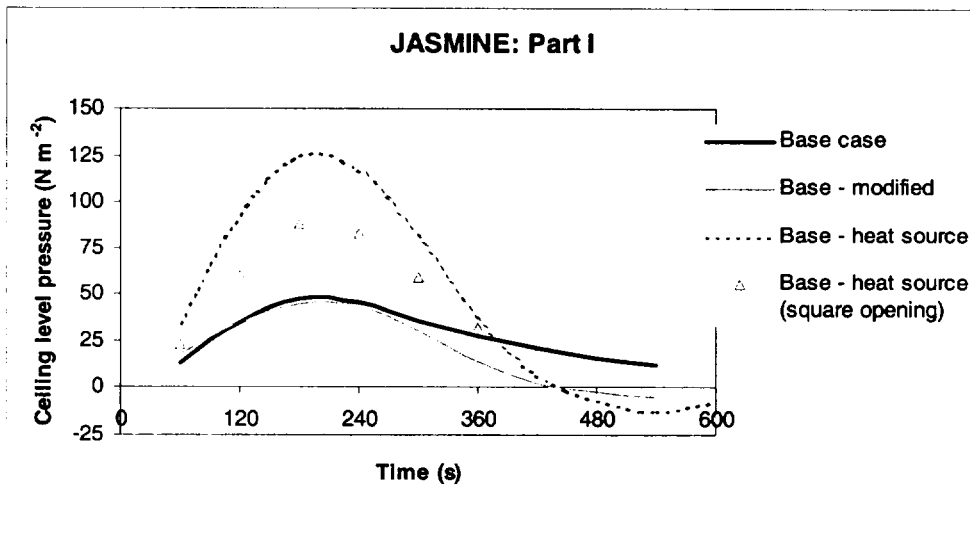


Figure 12 JASMINE predictions of pressure in Part I

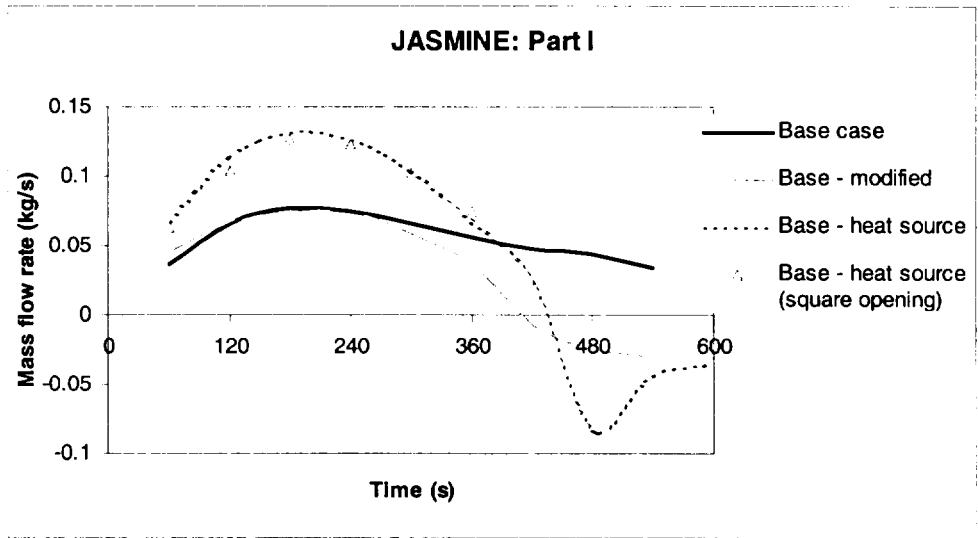


Figure 13 JASMINE predictions of inflow/outflow in Part I

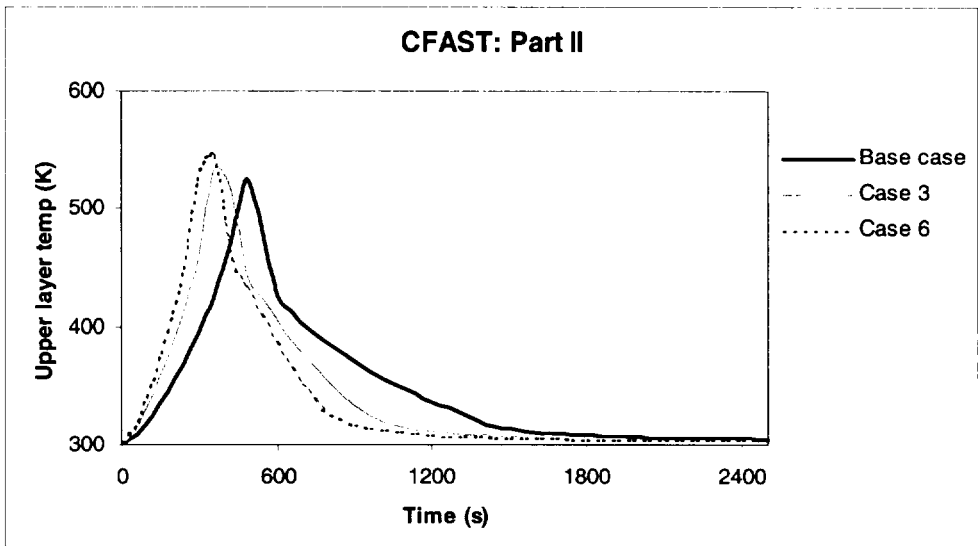


Figure 14 CFAST predictions of upper layer temperature in Part II

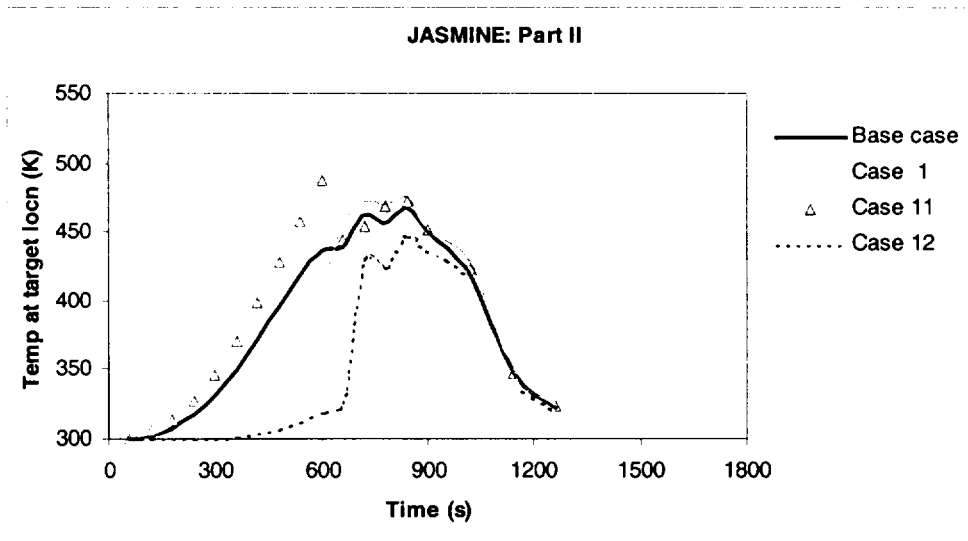


Figure 15 JASMINE predictions of gas temperatures in Part II

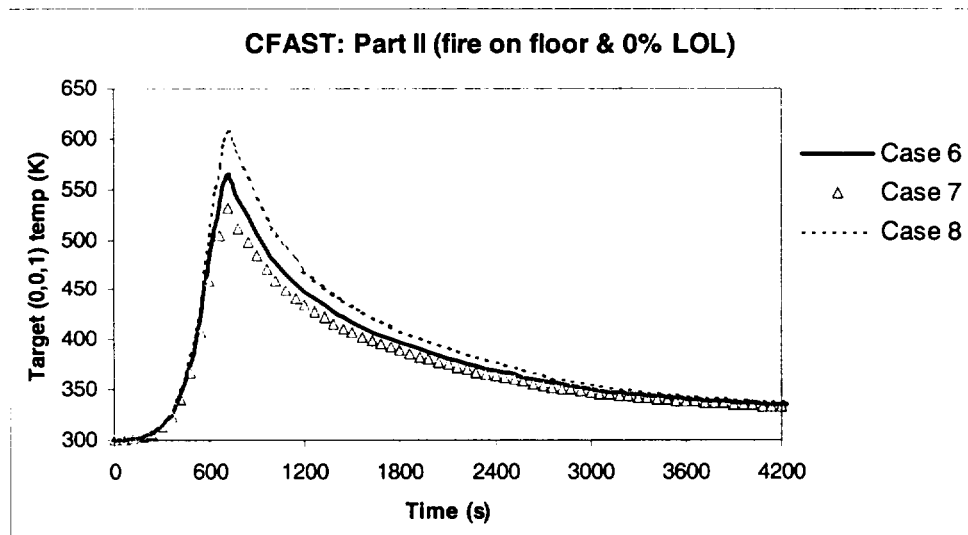


Figure 16 CFAST predictions of target temperatures in Part II

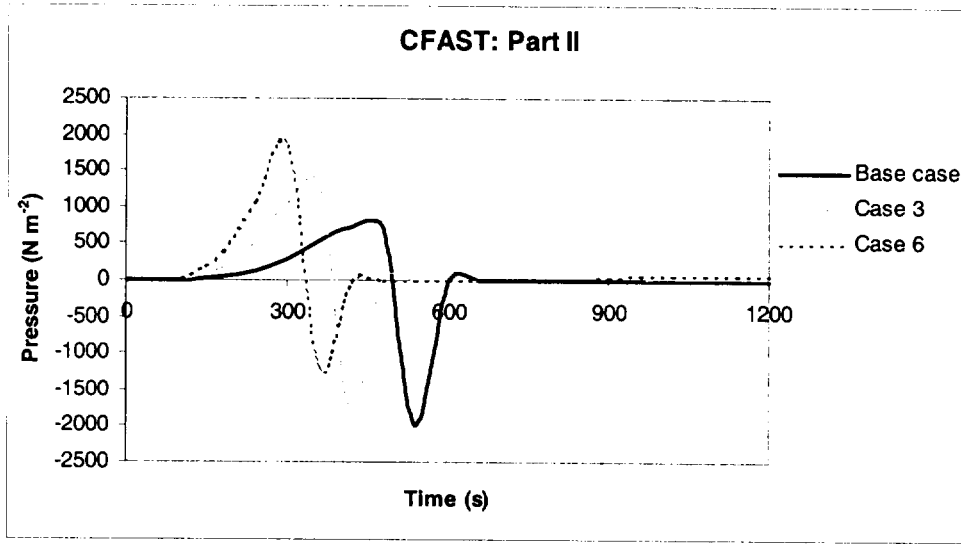


Figure 17 CFAST predictions of pressure in Part II

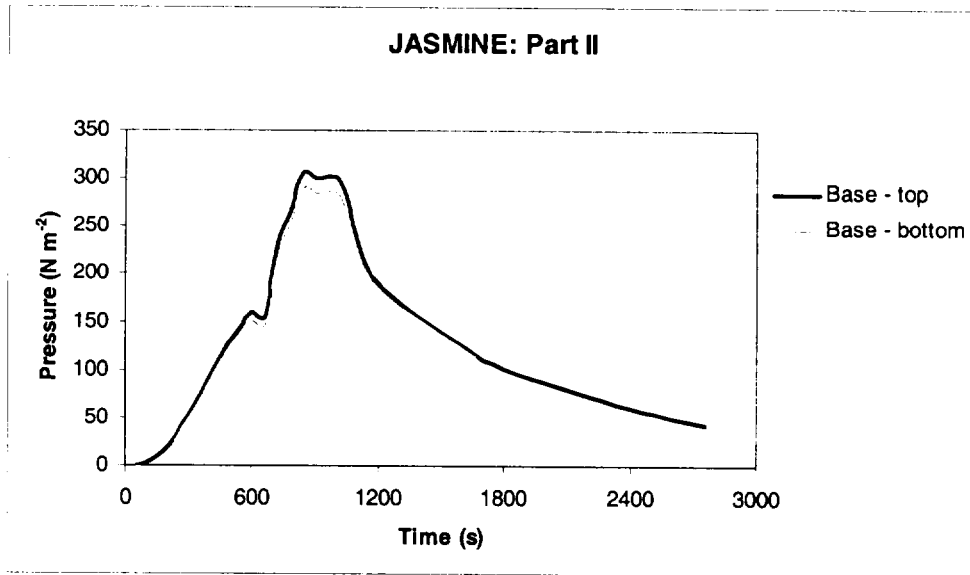


Figure 18 JASMINE predictions of pressure in Part II

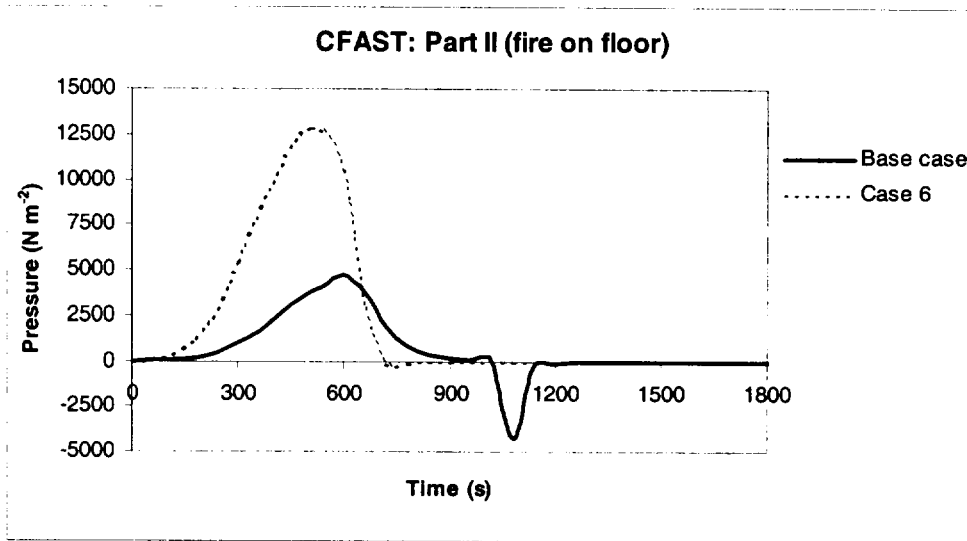


Figure 19 CFAST predictions of pressure in Part II

CONCLUDING REMARKS

BRE simulations of the benchmark exercise with JASMINE and CFAST indicate that target cable damage is unlikely for either Part I or Part II. In Part I this is a consequence of the small fire size, while for Part II with the bigger fires the effect of oxygen depletion was important. Although the temperatures predicted by JASMINE and CFAST were broadly similar, the pressure predictions for the door crack cases were not. For Part II the over-pressure differed by a factor of two, while in Part I the CFAST predicted over-pressures were a factor of ten or more greater than for JASMINE. There are assumptions made in both models that may have a bearing. However the issue has not been resolved yet, and requires further consideration.

Some other important issues remain, in particular in respect to modelling the fluxes to the cable targets and the heat conduction within the target. Further work is required in developing conduction models for cable type targets, and the task of modelling radiation from the flaming region and hot gas layer to the target needs to be considered more carefully. Here the use of CFD models, in combination with appropriate radiation models, may offer significant benefit. Furthermore, to address properly the hazard associated with cable tray fires, some form of fire growth/spread model may be required. The assumption that the entire length of cable tray burns from the start of the fire under-estimates the potential the potential thermal damage to the target cable during the growing stage of the fire.

Although the results of the benchmark exercise would seem to provide confidence in using either zone or CFD models to that type of scenario, it is felt that the problem of 'nearly-sealed' compartments needs further thought. The particular cases studied may have masked the potential problems associated with such scenarios since other effects such as oxygen depletion were here more important. However, in another situation the degree of pressure build-up, and the associated venting and reverse-venting of air, may be more crucial.

The next stage of the collaborative project will need to consider more carefully the limits of fire models for other types of scenario. Here, issues such as the limitation of zone models for very large or complex geometries, or the presence of complex mechanical ventilation systems, need addressing.

REFERENCES

1. MaCaffrey B.J. "Momentum implications for buoyant diffusion flames", *Combustion and Flame*, Vol 52, 1983, p 149.
2. Siegel R. & Howell J.R. *Thermal Radiation Heat Transfer*, Hemisphere Publishing Corporation, New York, 2nd ed., 1981.
3. Peacock R.D. et al. "A User's Guide for FAST: Engineering Tools for Estimating Fire Growth and Smoke Transport", Special Publication 921, NIST, U.S. Dept of Commerce, 2000.
4. Peacock R.D. et al. "CFAST, the Consolidated Model of Fire Growth and Smoke Transport", NIST Technical Note 1299, NIST, U.S. Dept of Commerce, 2000.
5. Ferziger J.H. & Perić M. "Computational methods for fluid dynamics – 2nd ed.", Springer, 1999.
6. Versteeg H.K & Malalasekera W. "An introduction to computational fluid dynamics – the finite volume method", Addison Wesley Longman, 1995.
7. Patankar S.V. "Numerical heat transfer and fluid flow", Hemisphere Publishing Co., 1980.
8. Launder B.E. & Spalding D.B. "The numerical computation of turbulent flows", *Computer Methods in Applied Mechanics and Engineering*, vol. 3, 1974, pp 269-289.
9. Markatos N.C., Malin M.R. & Cox G. "Mathematical modelling of buoyancy induced smoke flow in enclosures", *Int. J. Heat Mass transfer*, vol. 25, 1982, pp 63-75 (and letter on above: vol. 25, 1982, pp 1777-1778).
10. Patankar S.V. & Spalding D.B. "A calculation procedure for heat, mass and momentum transfer in three-dimensional parabolic flows", *Int. J. Heat Mass Transfer*, vol. 15, 1972, p 1787.
11. Magnussen B.F. & Hjertager B.H. "On mathematical modelling of turbulent combustion with special emphasis on soot formation and combustion", *Proceedings of the 16th Symposium (International) on Combustion*, The Combustion Institute, 1976, pp 719-729.
12. Gosman A.D. & Lockwood F.C. "Incorporation of a flux model for radiation into a finite-difference procedure for furnace calculations", *Proceedings of the 14th Symposium (International) on Combustion*, The Combustion Institute, 1973, pp 661-671.
13. Lockwood F.C. & Shah N.G. "A new radiation solution method for incorporation in general combustion prediction procedures", *Proceedings of the 18th Symposium (International) on Combustion*, The Combustion Institute, 1981, pp 1405-1414.
14. Truelove J.S. "Mixed grey gas model for flame radiation", UK Atomic Energy Authority Report AERE HL 76/3448, 1976.
15. Kumar S., Gupta A.K. & Cox G. "Effects of thermal radiation on the fluid dynamics of compartment fires", *Fire Safety Science – Proceedings of the Third International Symposium*, Elsevier Science Publishing, 1991, pp 345-354.
16. Cox G. & Kumar S. "Field modelling of fire in forced ventilated enclosures", *Combustion. Science and Technology*, vol. 52, 1987, pp 7-23.

17. Cox G., Kumar S. & Markatos N.C. "Some field model validation studies", Fire Safety Science – Proceedings of the First International Symposium, Hemisphere Publishing, 1986, pp159-171.
18. Pericleous K.A., Worthington D.R.E. & Cox G. "The field modelling of fire in an air-supported structure", Fire Safety Science – Proceedings of the Second International Symposium, Hemisphere Publishing 1989, pp 871-880.
19. Kumar S. & Cox G. "The mathematical modelling of fires in road tunnels", Proc. 5th International Symposium on the Aerodynamics & Ventilation of Vehicle Tunnels, Lilie, France, BHRA, 1985, pp 61-76.
20. Kumar S. & Cox G. "Radiant heat and surface roughness effects in the numerical modelling of tunnel fires", Proc. 6th International Symposium on the Aerodynamics & Ventilation of Vehicle Tunnels, Durham, England, BHRA, 1988, pp 515-526.
21. Miles S., Kumar S. & Andrews R. "Validation of a CFD model for fires in the Memorial Tunnel", Proc. 1st International Conference on Tunnel Fires, Lyon, France, Independent Technical Conference, 1999, pp 159-168.
22. Kumar S. "Field model simulations of vehicle fires in a Channel Tunnel shuttle wagon", Fire Safety Science – Proceedings of the Fourth International Symposium, IAFSS, 1994, pp 995-1006.
23. Kumar S., Welch S. & Chitty R. "Evaluation of fire models for fire hazard assessment in buildings. Part 2 – evaluation of fire models", BRE Client Report 75982, 1999.
24. Miles S. "The predictive capability of CFD for fully developed fires", Proc. 3rd International Symposium on Fire and Explosion Hazards, Windermere, UK, 2000.
25. Miles S.D., Kumar S. & Cox G. "Comparisons of 'blind predictions' of a CFD model with experimental data", Fire Safety Science – Proceedings of the Sixth International Symposium, IAFSS, 2000, pp 543-554.
26. Miles S., Kumar S. & Cox G. "The balcony spill plume – some CFD simulations", Fire Safety Science – Proceedings of the Fifth International Symposium, IAFSS, 1997, pp 237-247.
27. Kumar S., Heywood G.M. & Liew S.K. "Superdrop modelling of a sprinkler spray in a two-phase CFD-particle tracking model", Fire Safety Science – Proceedings of the Fifth International Symposium, IAFSS, 1997, pp 889-900.

**Appendix H: Benchmark Analysis with CFAST,
Juergen WILL, GRS, Germany**

Report

Benchmark Exercise #1 Cable Tray Fires of Redundant Safety Trains

**Blind Simulations using
CFAST 4.0.1**

International Collaborative Project to Evaluate Fire Models for Nuclear Power Plants

May 23, 2001

Contens

1	Computer Code	4
2	Benchmark Exercise Part I	4
2.1	Input Data for Part I	4
2.2	Results of Part I	5
2.2.1	Distance between tray A and trash bag (base case and cases 1 - 3)	5
2.2.2	Ventilation conditions (base case, cases 4 and 5)	10
3	Benchmark Exercise Part II	22
3.1	Input data for Part II	22
3.2	Results of Part II	23
3.2.1	Heat release rate	23
3.2.2	Layer temperatures and interface height	25
3.2.3	Mass flow rate of mechanical ventilation system and through the opened door	34
3.2.4	Target surface temperature	37
4	Conclusions	41

1 COMPUTER CODE

All calculations were performed applying the multi-room zone model CFAST [1], most actual version 4.0.1. The older Version 3.1.6 could not be used because all available personal computers (PCs) were running under Microsoft WINDOWS NT operation system. Testing CFAST version 3.1.6 on a WINDOWS 98 platform also failed. PCs (without hardware handicaps) with WINDOWS 95 operational system were not available.

All the information referring to the model or the computer code was taken from

- NIST TN 1431: A technical reference for CFAST: An engineering tool for estimating fire and smoke transport. January 2000, [1],
- NIST Special Publication 921 2000 Edition: A user's guide for FAST: Engineering tools for estimating fire growth and smoke transport. January 2000, [2],
- NIST Technical Note 1299: CFAST, the consolidated model of fire and smoke transport. September 1995, [3]
- personal information given by Mr. G. Blume (iBMB of TU Braunschweig), who performed a lot of calculations with CFAST 3.1.6 in the past.

In our opinion it does not make a strong difference whether CFAST version 3.1.6 or version 4.0.1 is used. Comparing the manuals of these two program versions, no changes in the physical basis were found. Applying the more actual version does not seem to be as comfortable as the older one because the graphic user interface (GUI) FAST is no longer available and creating an input data file is a little more difficult.

2 BENCHMARK EXERCISE PART I

2.1 INPUT DATA FOR PART I

All the information was taken from "Benchmark Exercise #1: Cable Tray Fires of Redundant Safety Trains", revised September 11, 2000, [4].

The thermophysical data for walls, floor and ceiling as well as for the PVC insulation material of the cables were put in a new file THER_ST.DF as well as THER_ST.NDX. The cable of tray A was described on the one hand as a target, on the other hand as an object. Using the object model, a set of new files (OBJE_ST.DF, OBJE_ST.NDX) for the object properties was set up.

In each case of part I tray A was treated as an object or as a target. Preliminary calculations had shown that there is a considerable difference in the results using the unconstrained or the constrained fire algorithm. Therefore, these two algorithms were used in the calculations of the base case and of the cases 1 to 5. These two additional parameters lead to four different calculations for each case.

2.2 RESULTS OF PART I

2.2.1 Distance between tray A and trash bag (base case and cases 1 - 3)

From the base case up to case 3 the fire as well as the ventilation conditions were not changed. Therefore, it is obvious that the temperature of the upper and the lower layer, the depth of hot gas layer, the heat release rate and the oxygen content did not change either. The time curves of these parameters are shown in Figure 2.1 - Figure 2.5.

The course of the parameter describing the fire itself or the upper and lower layer is not affected by using different models (object or target) for tray A.

Starting the calculations, it was expected that in case of using constrained fire algorithm (fire type 2) the heat release rate is limited by oxygen consumption. But this did not happen, the heat release rate of the main fire (trash bag) is not affected by lack of oxygen (Figure 2.4). The oxygen content in the lower layer is not reduced by the trash bag fire (Figure 2.5). In the upper layer, there is a high amount of oxygen until the end of the simulation time, too.

Although it is not mentioned in the CFAST manuals, the two types of fire lead to totally different results with respect to the layer temperatures. Using the constrained fire algorithm, much higher upper and lower layer temperatures were calculated. This is surprising, because the interface height did not seem not to be affected (Figure 2.3) by the fire algorithm. But most surprising is the fact that in all runs of the program the surface temperature of tray A (as well as ceiling, walls and floor) is higher if the unconstrained fire algorithm is used, resulting in a lower gas temperature (Figure 2.6). For the analyst, it seems that something went wrong in calculating the convective and radiative heat flux on the target surface. Maybe in case of the unconstrained fire absorption by carbon dioxide and water vapour in the gas layers is ignored: Without absorption the layers do not heat up as much and the radiative heat flux on the ceiling, walls, floor and targets is higher, so that the surface temperature increases.

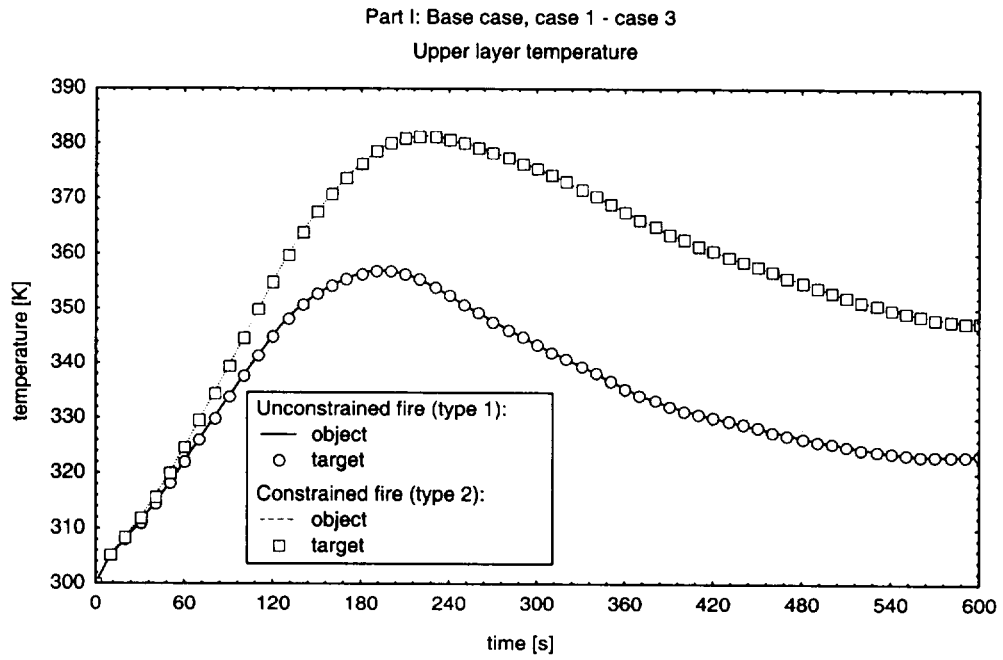


Figure 2.1 Upper layer temperature (base case, cases 1 - 3)

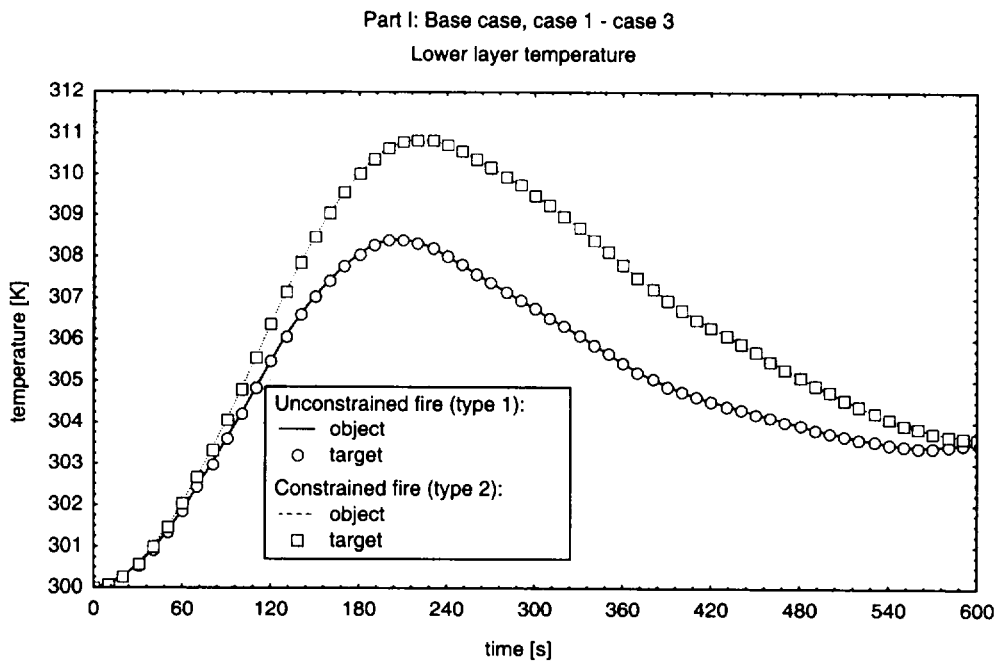


Figure 2.2 Lower layer temperature (base case, cases 1 - 3)

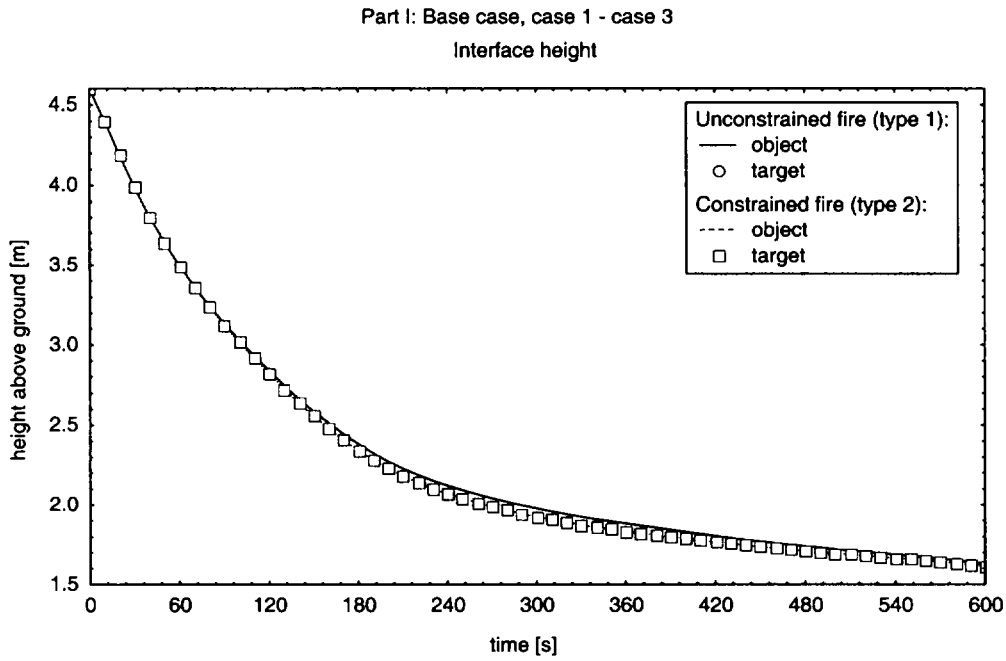


Figure 2.3 Interface height (base case, cases 1 - 3)

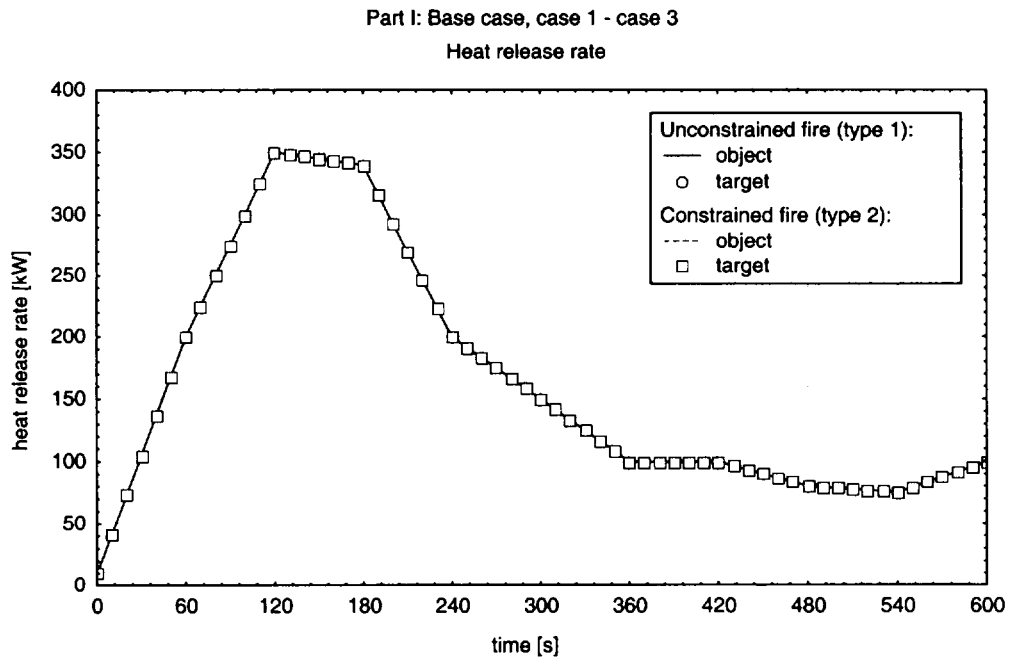


Figure 2.4 Heat release rate (base case, cases 1 - 3)

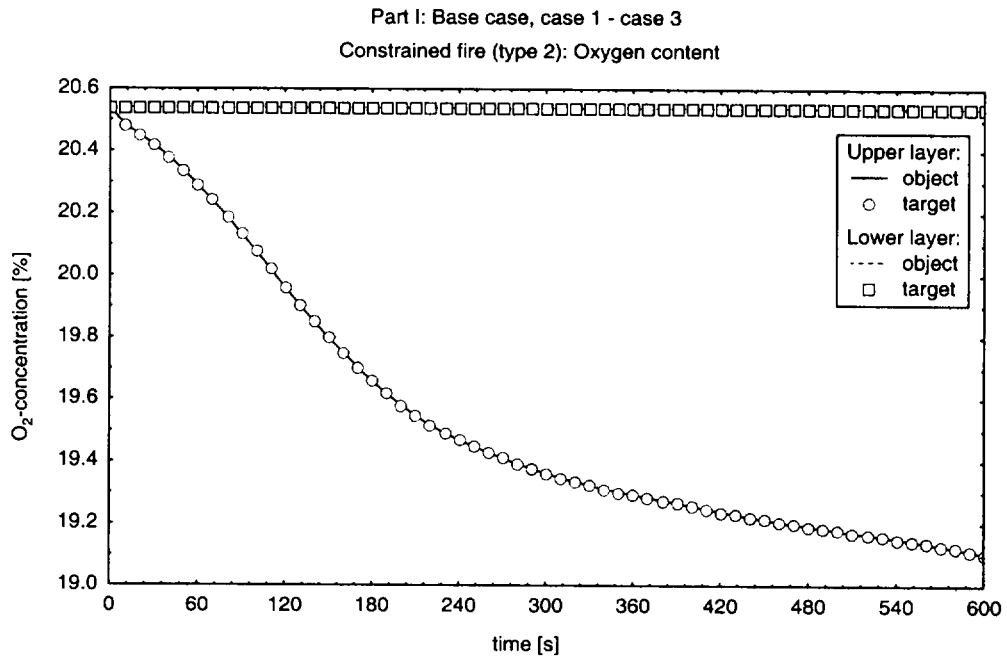


Figure 2.5 Oxygen content (base case, cases 1 - 3)

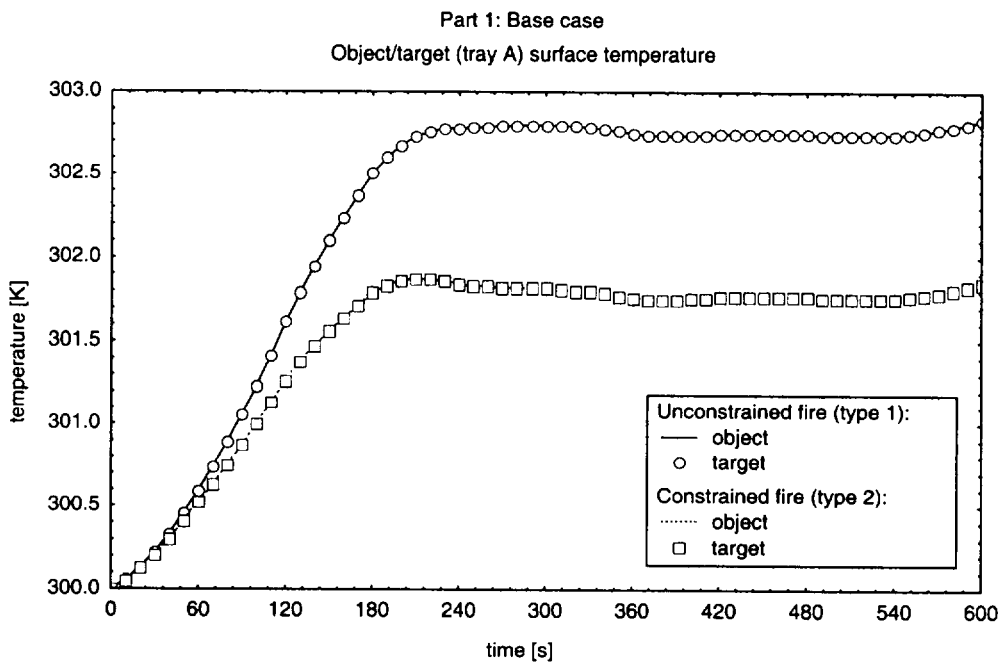


Figure 2.6 Surface temperature of tray A (base case)

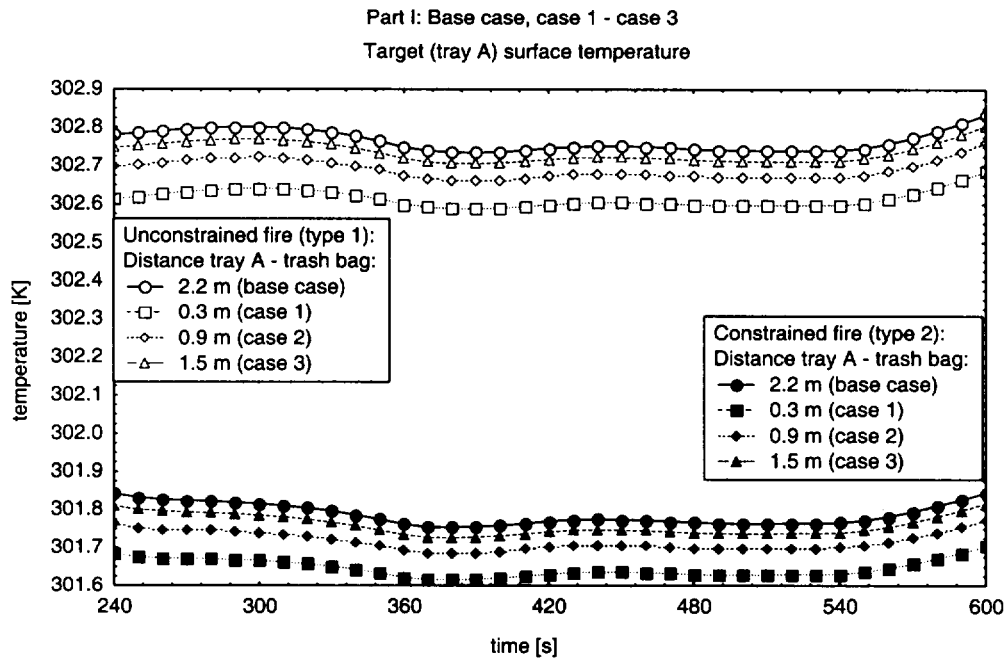


Figure 2.7 Surface temperature of tray A, unconstrained fire (base case, cases 1 - 3)

Comparing the surface temperature of tray A for different distances between the main fire (trash bag) and the target (base case, cases 1 - 3) is more amazing: Increasing the distance between target and heat source leads to an increase of the surface temperature (Figure 2.7), the opposite was expected.

As originally the x-position of the target (tray A) was fixed and the position of the main fire (trash bag) was moved in x-direction, further calculations were performed to find out what has gone wrong: Using the unconstrained fire algorithm (type 1), defining the door closed and the ventilation system switched off, the main fire (trash bag) was fixed in the center of the room (x-position 4.55 m), and the target (tray A) was moved in x-direction to get the distance of 2.2 m, 0.3 m, 0.9 m and 1.5 m between tray A and the trash bag. Looking at the results of these additional calculations (Figure 2.8), the amazing result is reasonable: The x- or y-position of a target does not affect the result of surface temperature, it was always treated as if it is positioned in the centre of the compartment. Only the position of the main fire (trash bag) will affect changes in the surface temperature of targets or objects. This weakness in the heat transfer model of CFAST is not mentioned in any manual. Due to this, in the former calculations the distance between tray A and trash bag was treated by the program as 1.15 m (base case), 3.05 m (case

1), 2.45 m (case 2) and 1.85 m (case 3), giving reasonable results for surface temperature (Figure 2.7) calculations.

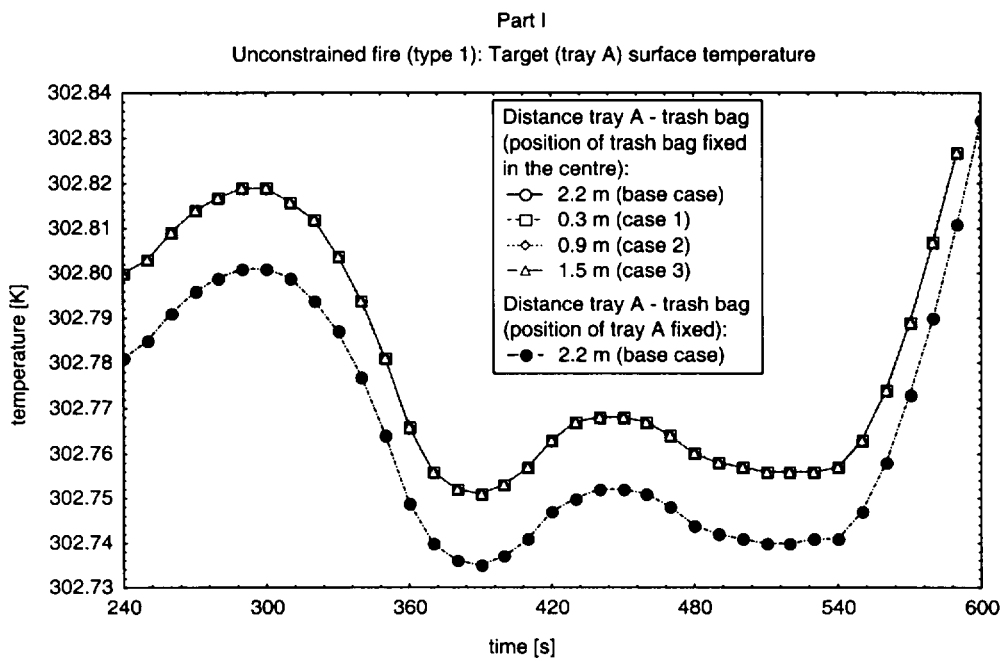


Figure 2.8 Surface temperature of tray A, constrained fire, position of trash bag fixed

2.2.2 Ventilation conditions (base case, cases 4 and 5)

The effects of different ventilation conditions should be shown by comparing the results of base case calculations and calculations with open door (case 4) or active ventilation system (case 5, case 5b).

It has been mentioned before that there have been some problems running CFAST with forced inflow (case 5). In this case, the oxygen content decreases until there is no more oxygen in the upper layer (Figure 2.9). It seems obvious that pure nitrogen was pumped into the compartment. There was no possibility in the input data file of CFAST to define the composition of the gas, which will be sucked in from the ambient into the compartment by a duct system. This problem did not appear in case of natural ventilation if the door is open (case 4). Thus the mechanical ventilation system was redefined: Concerning the following calculations, the outflow is managed by a fan and instead of the forced inflow a natural vent for horizontal flow is created to allow air to flow into the compartment (case 5b).

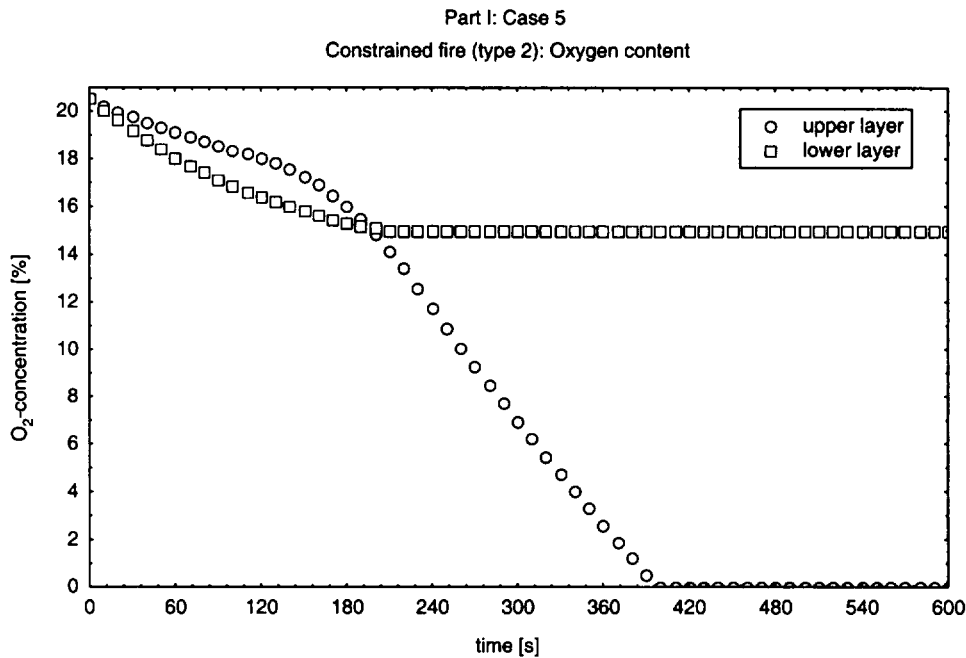


Figure 2.9 Oxygen content (case 5)

If an exchange of gases between the compartment and the ambient air is possible using openings as the door or a mechanical ventilation system, the temperature of the upper layer decreases nearly in the same magnitude (Figure 2.10, Figure 2.11). The increase in the lower layer temperature (Figure 2.12, Figure 2.13) and the decrease of the oxygen content in this layer are no longer important. Looking at the depth of the upper layer, which is not influenced by the fire type (Figure 2.14), and the oxygen content of this layer (Figure 2.15) it is discernible that the mechanical ventilation system (case 5b) is more effective than the natural ventilation by the open door (case 4). In case of the door opened or the mechanical ventilation system being active the surface temperature does not increase as much as without ventilation (Figure 2.16, Figure 2.17).

It has to be admitted that the increase of the oxygen concentration in the lower layer in case of an active ventilation (case 4, case 5b) is not reasonable. It has to be checked if the composition of ambient air and the air in the compartment at the beginning of the simulation are identical. It does not seem to be possible to define the gas composition in CFAST.

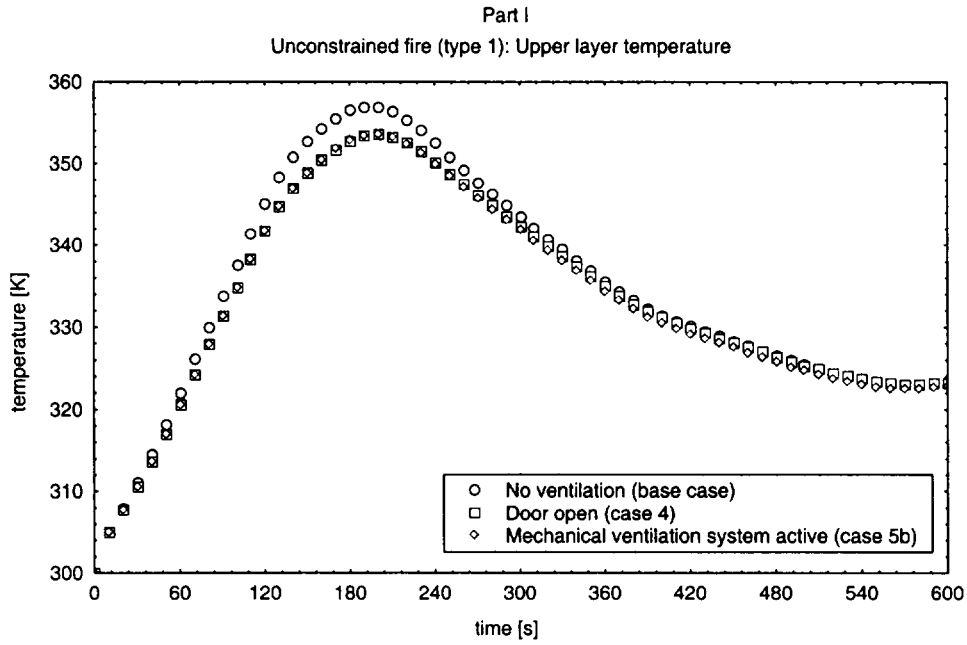


Figure 2.10 Upper layer temperature, unconstrained fire (base case, case 4, case 5)

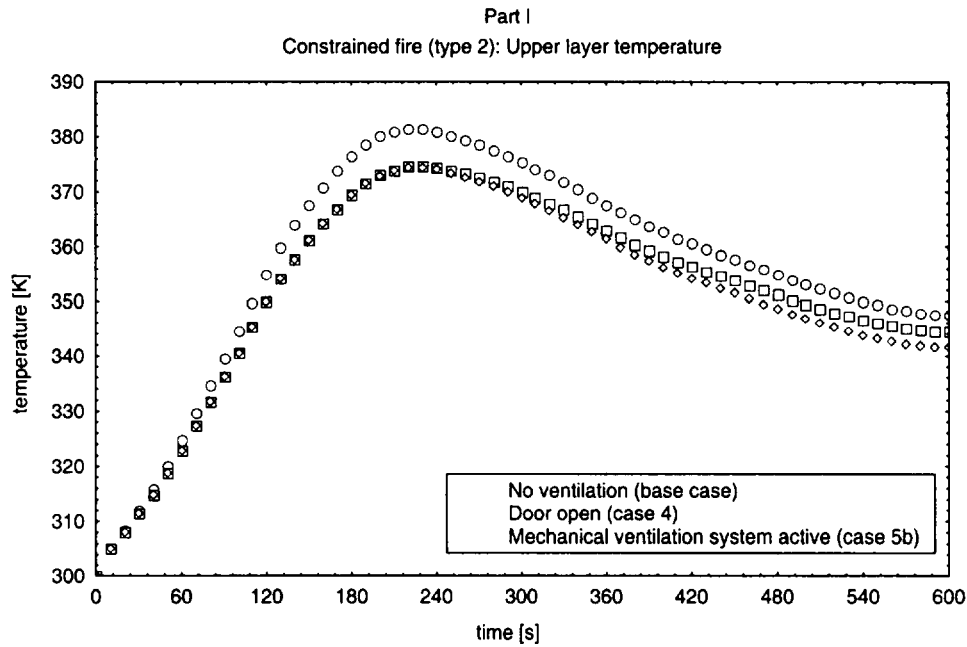


Figure 2.11 Upper layer temperature, constrained fire (base case, case 4, case 5)

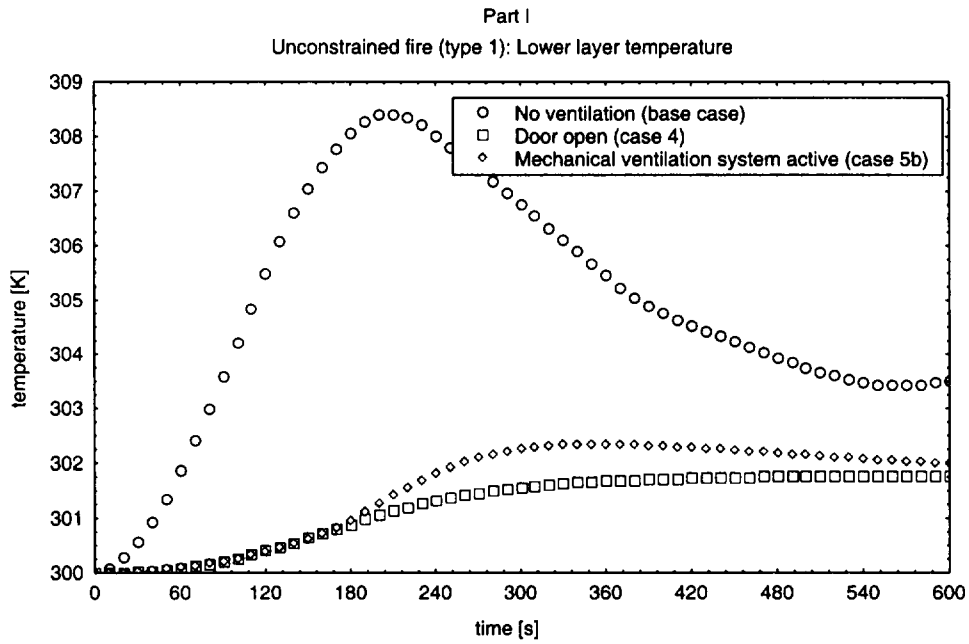


Figure 2.12 Lower layer temperature, unconstrained fire (base case, case 4, case 5)

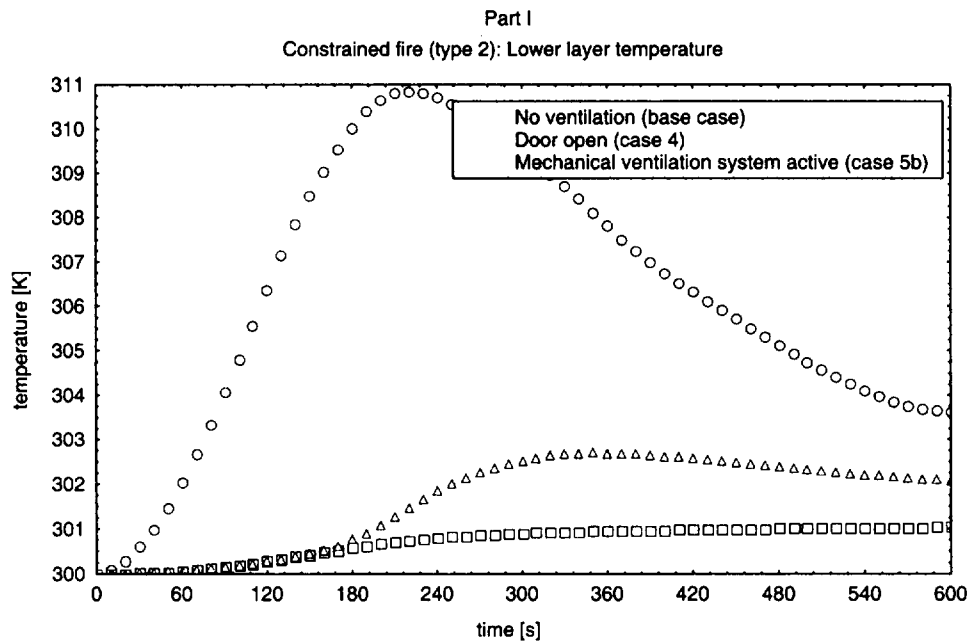


Figure 2.13 Lower layer temperature, constrained fire (base case, case 4, case 5)

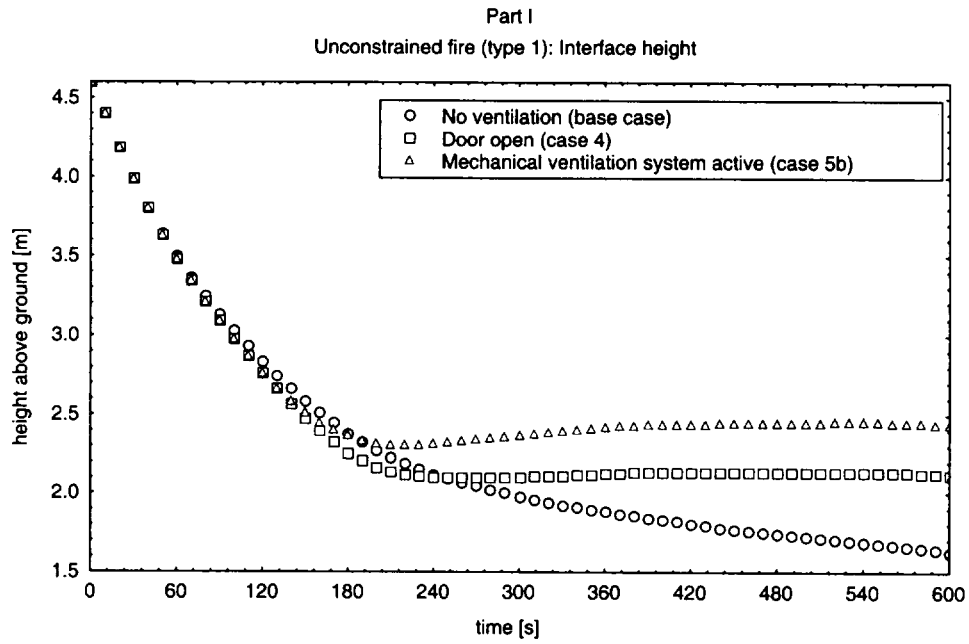


Figure 2.14 Interface height, unconstrained fire (base case, case 4, case 5)

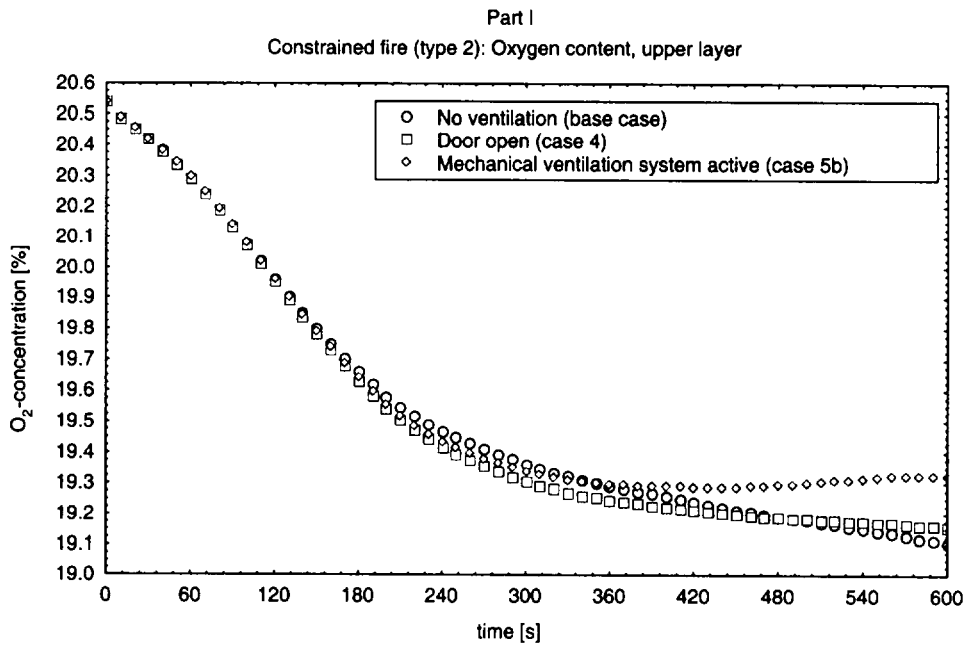


Figure 2.15 Oxygen content of upper layer (base case, case 4, case 5)

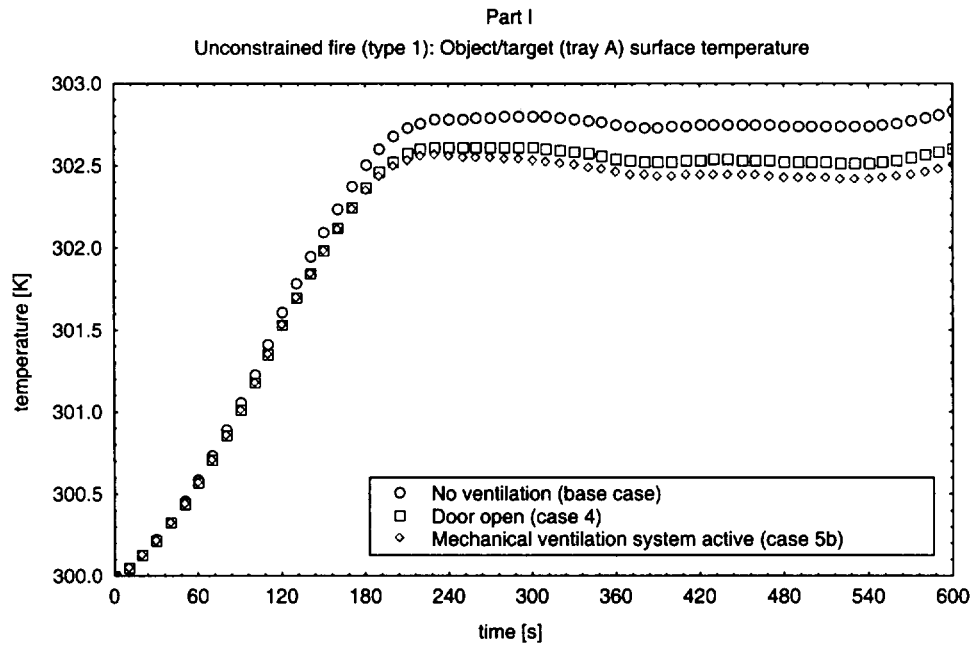


Figure 2.16 Surface temperature of tray A, unconstrained fire (base case, case 4, case 5)

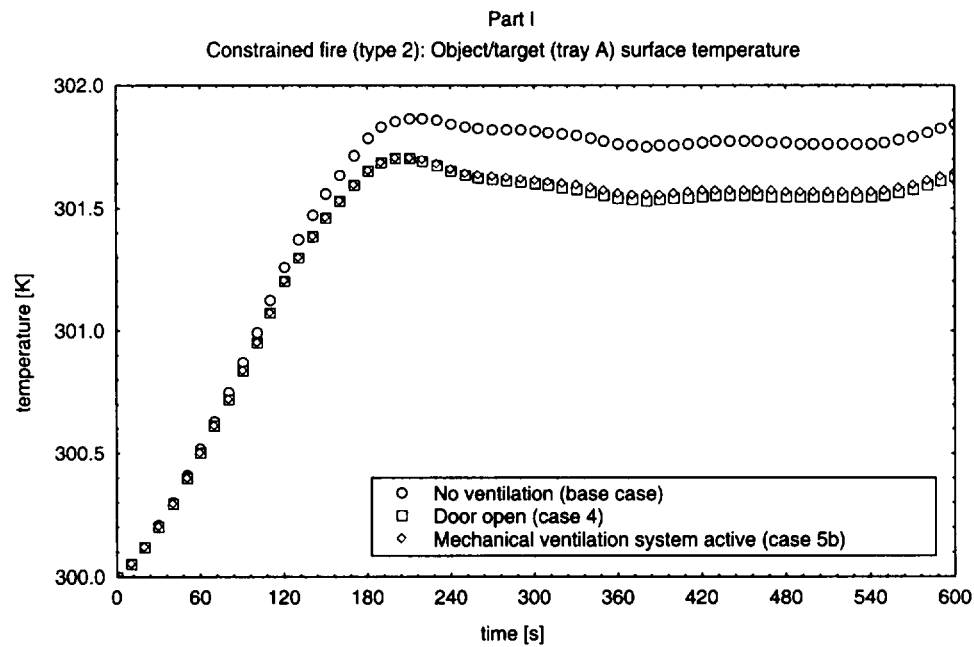


Figure 2.17 Surface temperature of tray A, constrained fire (base case, case 4, case 5)

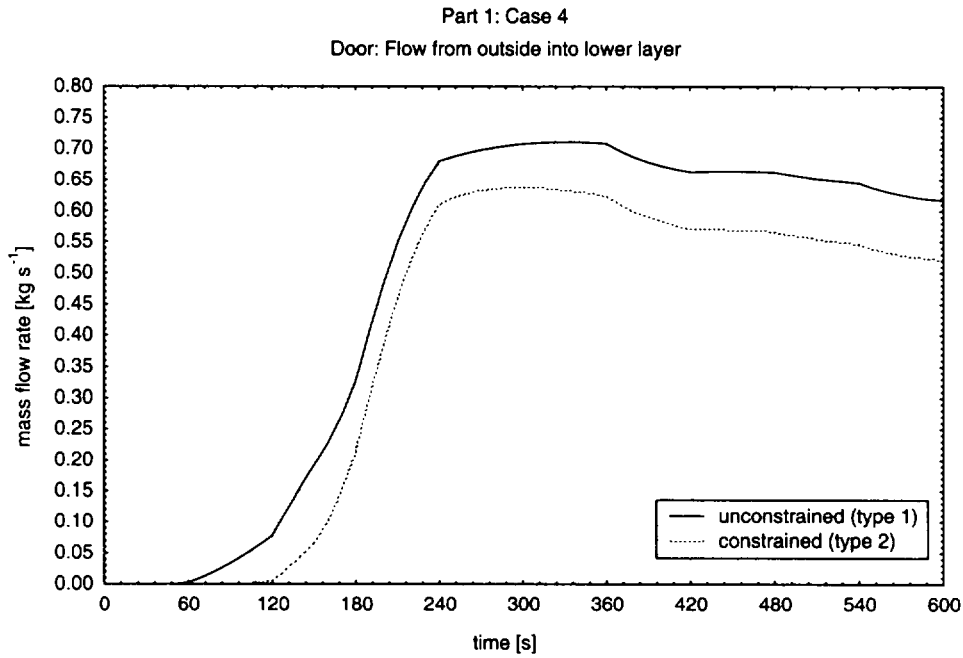


Figure 2.18 Mass flow rate through the opened door (outside - lower layer)

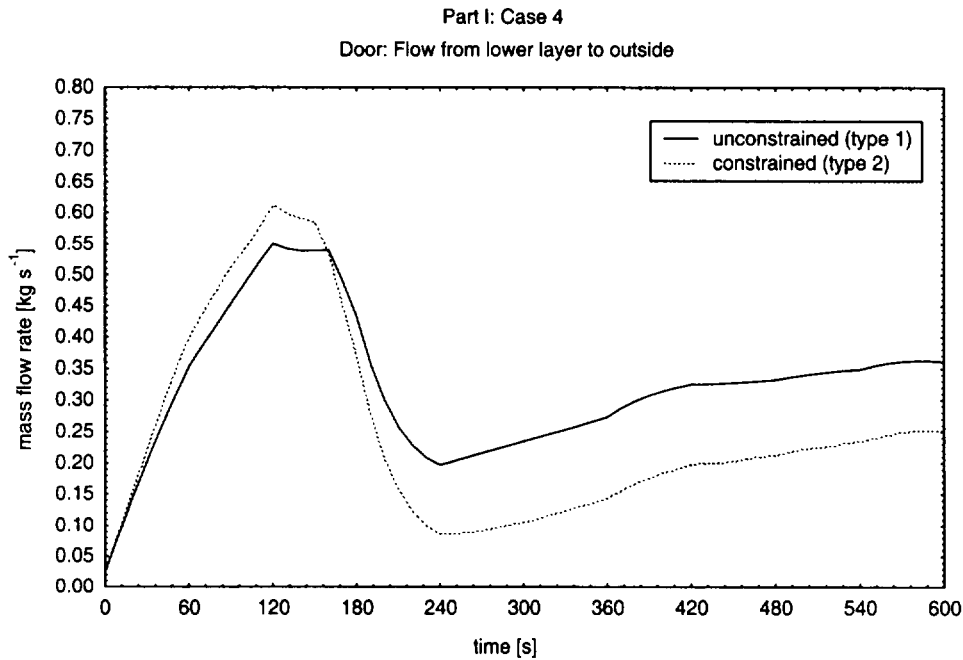


Figure 2.19 Mass flow rate through the opened door (lower layer - outside)

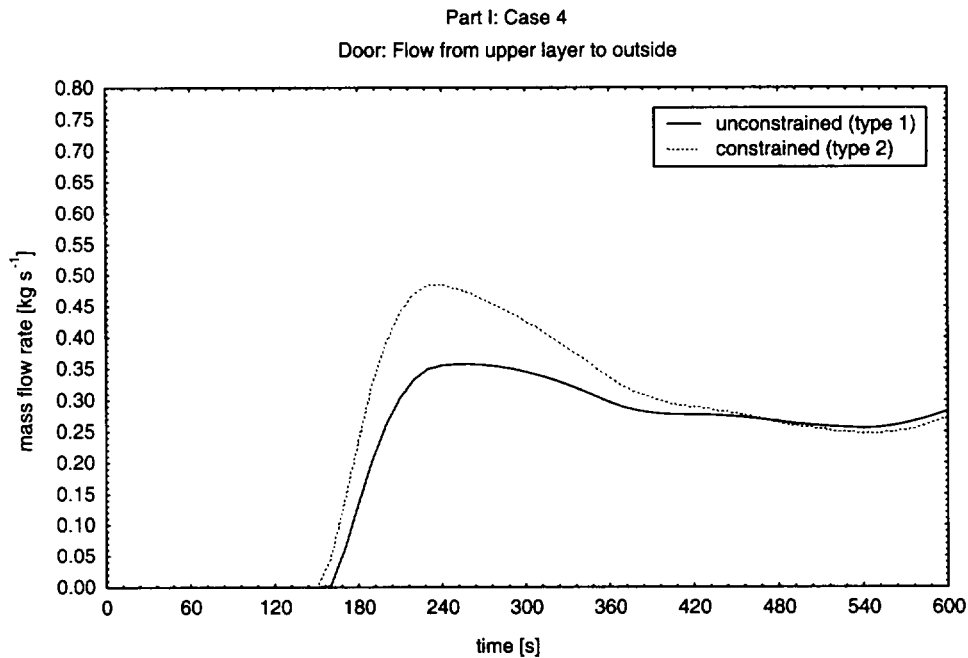


Figure 2.20 Mass flow rate through the opened door (upper layer - outside)

If the door of the compartment is opened (case 4), only lower layer gas flows out of the compartment. After approximately 2 minutes the interface reaches the top of the door, the gas flow from the upper layer to the outside starts, and the gas flow from the lower layer to the outside decreases (Figure 2.18, Figure 2.19, Figure 2.20).

In case 5b (mechanical ventilation system on but only for outflow, inflow by natural ventilation), the gas flows only in one direction through the opening (vent 1) from the outside into the lower layer (Figure 2.21). On the other hand, the fan sucks gas out of the lower layer until the interface reaches the bottom of the duct system opening. After that the fan sucks gas out of the upper layer.

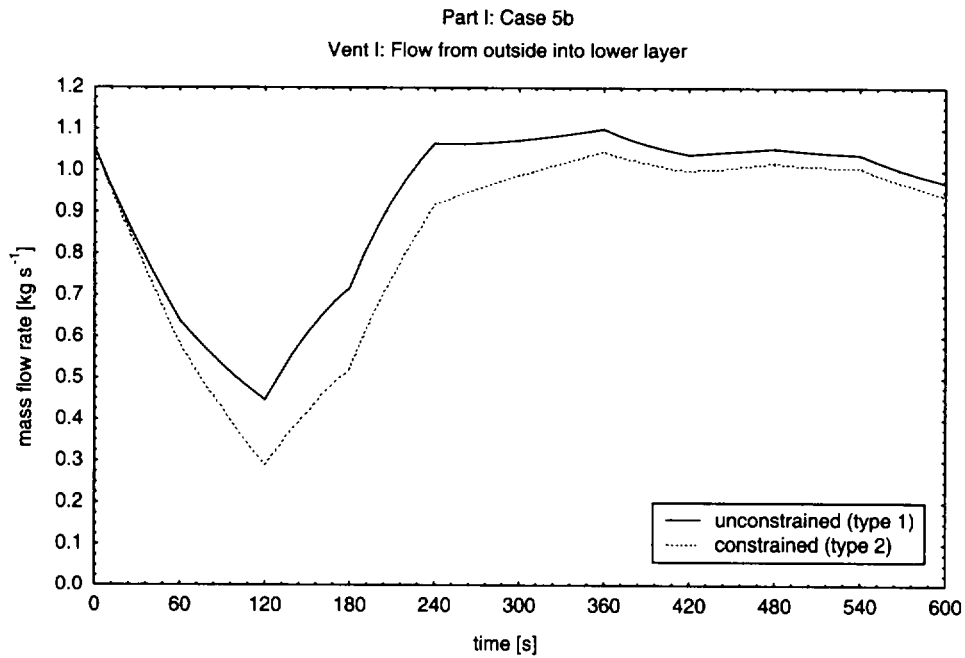


Figure 2.21 Mass flow rate through air inlet (outside - lower layer)

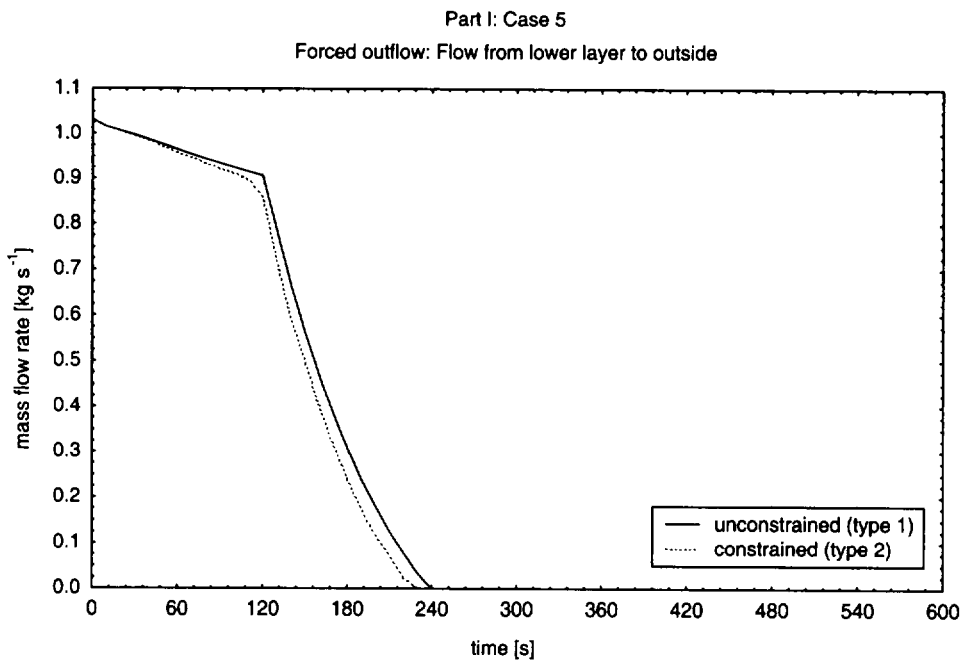


Figure 2.22 Mass flow rate of fan (lower layer - outside)

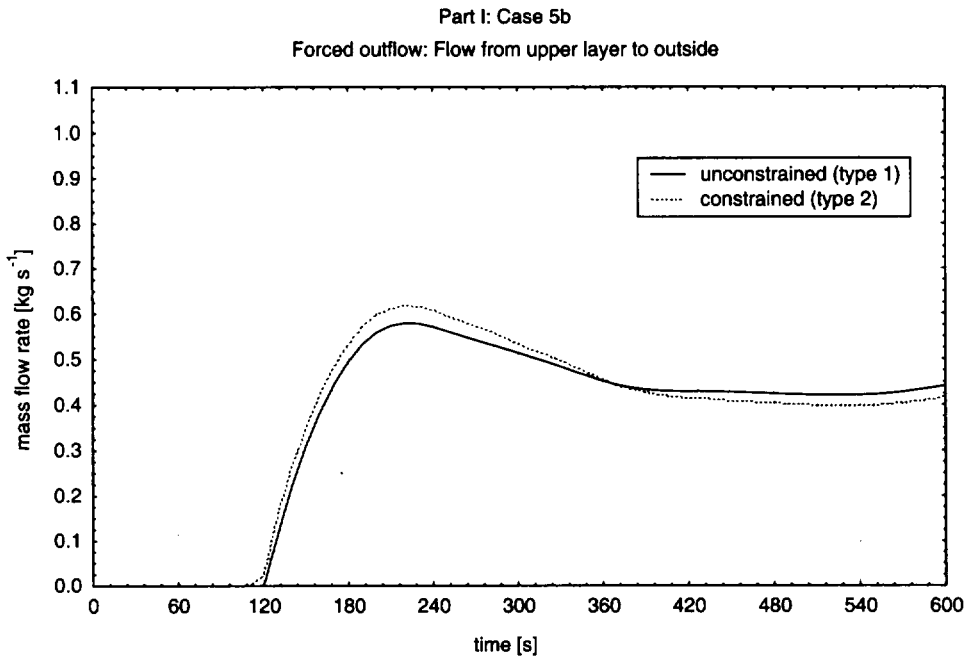


Figure 2.23 Mass flow rate of the fan (upper layer - outside)

Having a closer look at the pressure in the compartment it becomes visible that the base case is not realistic because the walls of the compartment (as well as the dampers of the ventilation system) have to resist a pressure of more than 10000 Pa (Figure 2.24). Even if a gap of 5 mm width under the door is assumed the pressure will reach a level of more than 1.000 Pa. If there is a sufficient ventilation area in the compartment like the open door (case 4), the pressure difference is very small (Figure 2.25). The pressure in the compartment hardly reaches the limitation of the fan in case of air being pumped into the room by a mechanical ventilation system (case 5), although another fan with the same sucks gas out of the compartment. (Figure 2.26). At least, if the mechanical ventilation system consists only of a fan sucking out gas and air flows into the compartment by natural ventilation (case 5b), the pressure inside the compartment is below atmospheric pressure (Figure 2.27).

In this context, it has to be pointed out that all results and statements are only valid in this special case of a very small fire of at least 350 kW heat release rate.

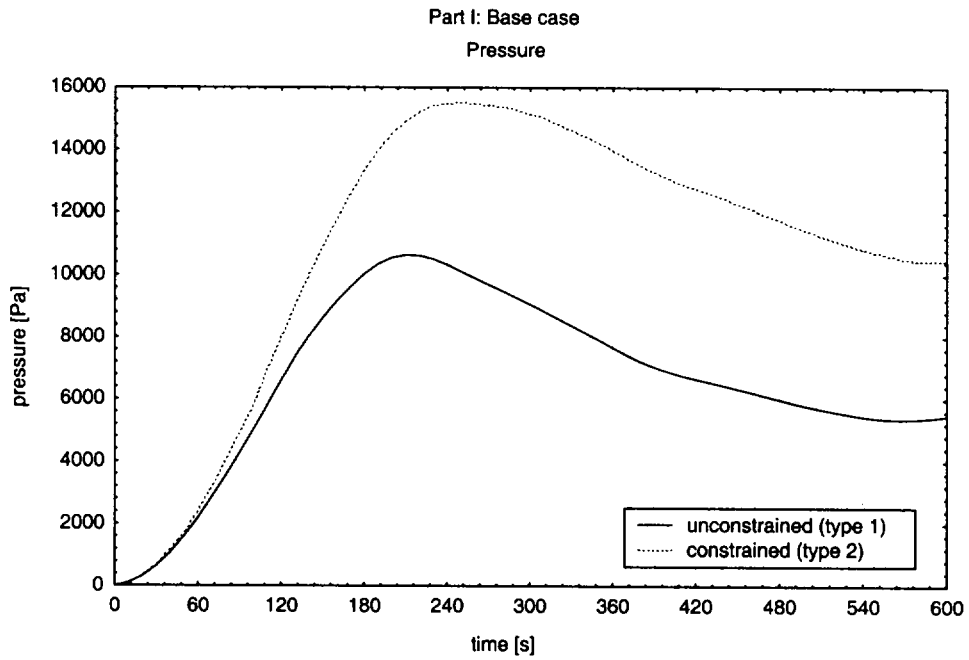


Figure 2.24 Pressure (base case)

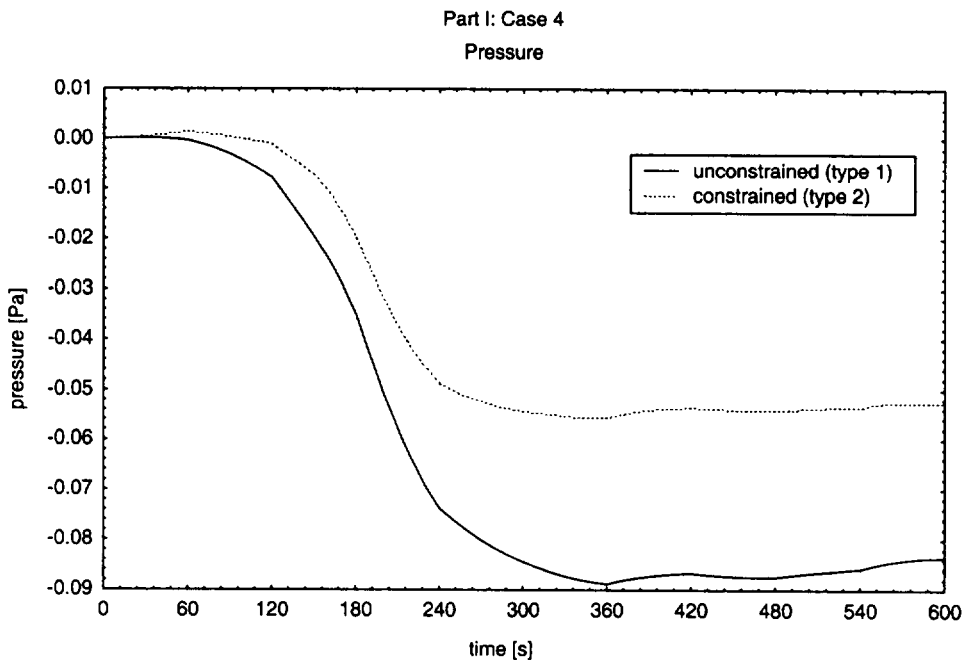


Figure 2.25 Pressure (case 4)

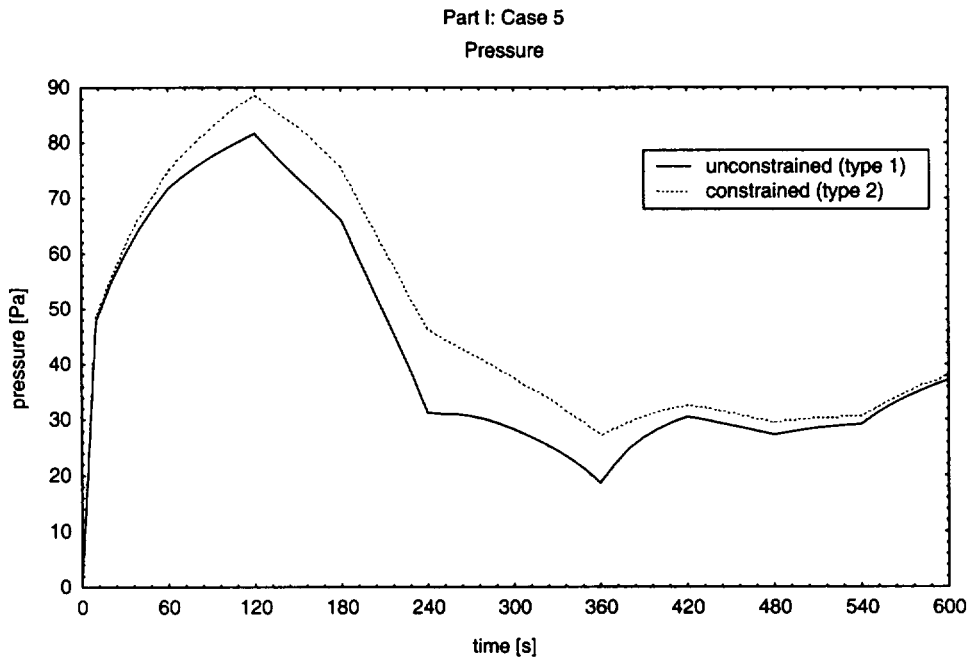


Figure 2.26 Pressure (case 5)

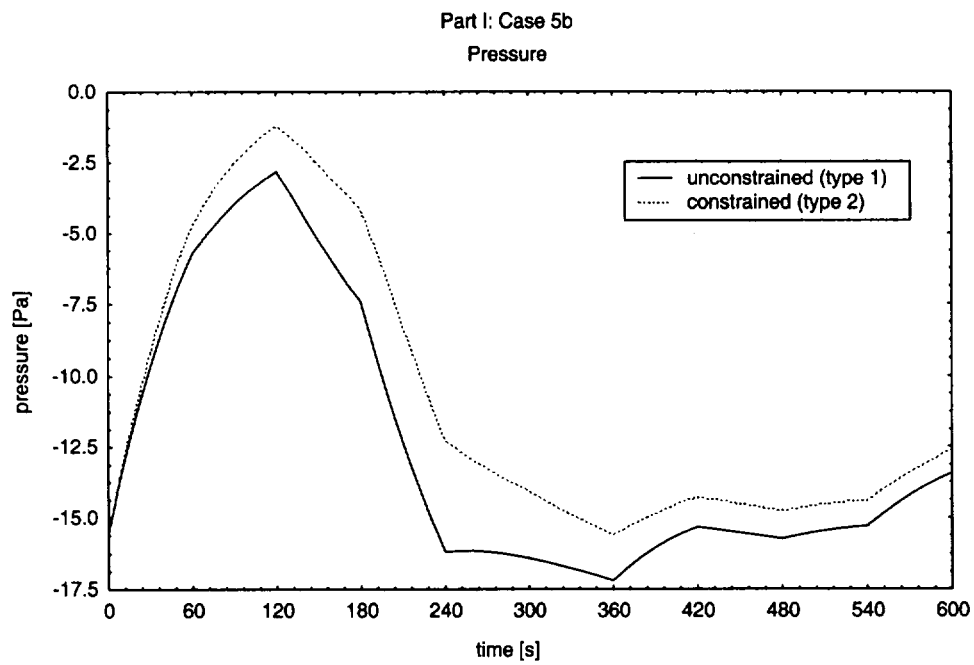


Figure 2.27 Pressure (case 5b)

3 BENCHMARK EXERCISE PART II

3.1 INPUT DATA FOR PART II

The thermophysical data for the walls, floor and ceiling as well as for the PVC cable insulation material were put in the former mentioned file THER_ST.DF as well as in the file THER_ST.NDX. As the heating of an object is treated like the heating of a target, only the object model of the files (OBJE_ST.DF, OBJE_ST.NDX) was used for cable tray B in part II. In all examined cases of part II both fire algorithms (unconstrained, constrained) were used. Using fire type 2 (constrained fire, the time curves of variables HCl, HCr, OD and CO were additionally specified. CFAST cannot treat a variable position of an object or target in the horizontal plane, therefore it was assumed that the object / target (tray B) was positioned in the center of the compartment and the main fire (tray A, C1, C2) was moved in y-direction to get the distances of 6.1 m, 4.6 m or 3.1 m (not in x-direction, because the compartment is not wide enough).

The mechanical ventilation system in case 9a and case 10 was defined in the same way as in case 5b of part I. To run the simulations for case 9, the variable CVENT was used, and two points were added to the time curve of the 1 MW cable fire.

The user of CFAST is not able to specify the volume flow rate of a forced ventilation (an option, which is included in the older zone model HARVARD 6) or to specify the capacity of a mechanical ventilation system as a function of time. Trying to run a simulation for a problem time of up to 15 min (with mechanical ventilation system being active and door closed) creates a restart file for this point of time. A restart of the simulation with a modified input data file (switch off mechanical ventilation system and door open) also failed. Therefore, case 9 was calculated on the one hand with mechanical ventilation (called case 9a) and without a mechanical ventilation system (called case 9b) on the other hand, while the door is opened after 15 min simulation time.

To run case 13, the file OBJE_ST.DF was modified: Instead of a panel thickness of 50 mm (third value in line 3) a thickness of 15 mm was applied to simulate a typical NPP specific instrumentation cable. Since the variations of the object elevation or thickness did not effect the surface temperature, case 11 to case 13 will not be mentioned anymore.

3.2 RESULTS OF PART II

3.2.1 Heat release rate

Using the unconstrained fire algorithm (type 1) the heat release rate reached the predicted level of 1 MW, 2 MW or 3 MW (Figure 3.1). On the other hand, if the constrained fire algorithm was used, the development of the heat release rate was limited by the position of the upper layer and the oxygen content of this layer.

Without natural or forced ventilation the heat release rate reached 1 MW (base case), stayed on this level for a short time period until there was no more oxygen in the upper layer. After that, the heat release rate decreased rapidly. A maximum value of about 1.3 MW was reached, although a peak heat release rate of 2 MW or 3 MW had been defined. After reaching this value the heat release rate decreased rapidly.

The heat release rate of the 1 MW fire was affected by opening the door after 15 min simulation time (Figure 3.2): The heat release rate did not increase as expected, but it decreased rapidly (base case - case 9b). More astonishing was the fact that the decrease of the heat release rate started earlier, if the mechanical ventilation system was active all the time (cases 9a, 10). This behaviour could be explained when looking at the position of the interface (Figure 3.15), which was a little bit deeper in case that the mechanical ventilation system was running and the main fire was placed in the pure oxygen layer at an earlier point of time.

In part I, the trash bag fire was very small (peak heat release rate of 350 kW) and did not last very long. In addition, the trash bag was positioned near the floor, so that the fire was in the lower layer and there was no lack of oxygen any time. In part II, the distance between floor and bottom of the main fire (cable fire of tray A, C1, C2) could influence the course of the heat release rate if the constrained fire algorithm (type 2) was used. To demonstrate this effect, base case (1 MW), case 5 (2 MW) and case 8 (3 MW) were modified so that the main fire was positioned on the floor ($z = 0.0$ m). Locating the fire on the floor even the peak heat release of 3 MW could be reached and kept for some minutes. If the fire was placed near the ceiling, it would be located inside the upper layer (with very low oxygen content) very soon and the fire development would slow down or stop. Therefore, a peak heat release rate of more than 1.3 MW could not be reached if the fire was placed 3.4 m above the floor. The course of heat release rate of main fire for the different cases is shown in Figure 3.3.

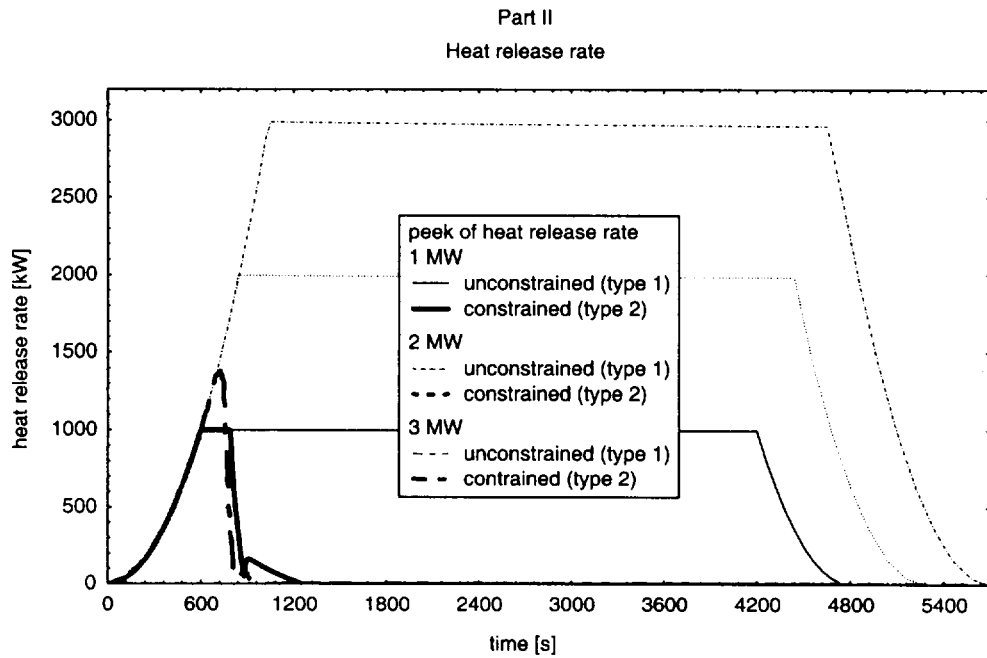


Figure 3.1 Effect of fire algorithm: Heat release rate

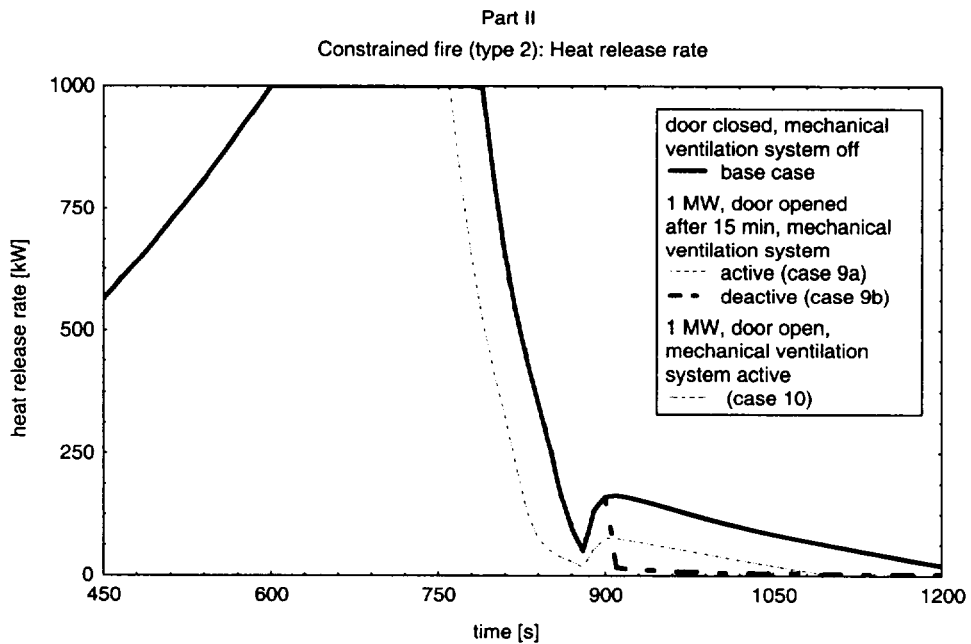


Figure 3.2 Effect of ventilation condition: Heat release rate

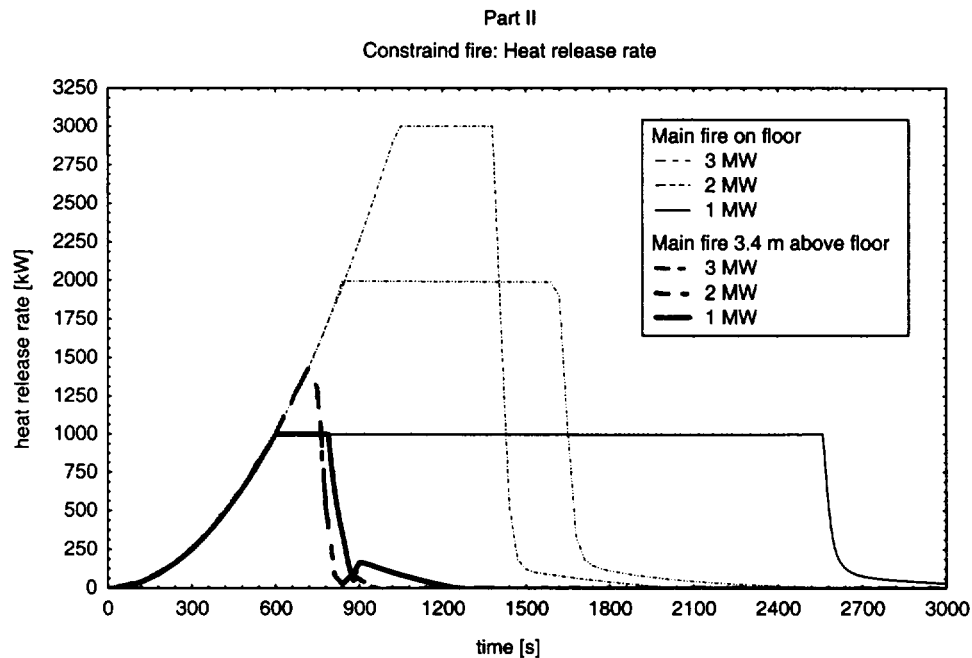


Figure 3.3 Effect of vertical fire position: Heat release rate

3.2.2 Layer temperatures and interface height

The distance between tray A, C1, C2 and tray B or the elevation of tray B do not affect the characteristics of the upper or lower layer. The temperatures of the layers and their thickness are mainly affected by the fire type, the heat release rate of the fire and the ventilation conditions.

Due to the fact that the fire growth is identical for the different cases of peak heat release rates (1 MW, 2 MW or 3 MW), the courses of the upper layer temperature (Figure 3.4, Figure 3.5), the lower layer temperature (Figure 3.6, Figure 3.7) and the interface height (Figure 3.8, Figure 3.9) are identical up to 600 s simulation time in all cases without any ventilation opening (base case - case 8, cases 11 - 13). Using the unconstrained fire algorithm (type 1), the course of these parameters runs simultaneously in case of a 2 MW fire and a 3 MW fire until a value of 2 MW is reached (840 s simulation time). The break in the course of the temperature and the interface height occurs earlier (750 s simulation time) if the constrained fire algorithm (type 2) is used. After reaching the break point (1 MW: 600 s, 2 MW: 840 s respectively 750 s), the temperature of the upper and the lower layer and the interface height develop in their own way in each different case of peak heat release rate.

To explain the influence of the ventilation conditions, the results of the 1 MW fire calculations (base case, cases 9a, 9b, 10) have to be compared. Looking at the course of the upper layer temperature (Figure 3.10, Figure 3.11), the ventilation conditions seem to have only a limited influence on the results. Obviously, the temperature of the lower layer is smaller if the door is open from the beginning and/or the mechanical ventilation system is active (Figure 3.12, Figure 3.13). The lower and upper layer cool down after 15 min simulation time if the door has been opened (base case - case 9b). In this case, there is also a discontinuity in the interface height (Figure 3.14, Figure 3.15). The lower layer temperature and the interface height do not differ if the door stays open all the time (case 10) or if it is opened after 15 min while the mechanical ventilation system has been active from the beginning (case 9a). Only the lower layer temperature grows a little bit higher if the door is closed at the beginning of the simulation and opened after 15 min (case 9b). The upper layer increases faster if the mechanical ventilation system is active all the time (case 9a, case 10).

The course of the upper layer temperature (Figure 3.16) is not affected by the fire algorithm used in the calculations until 600 s simulation time. But from 600 s until the point of time when a lack of oxygen occurs a faster increase of temperature is calculated using the constrained fire algorithm. This effect has also been observed in the simulations of part I.

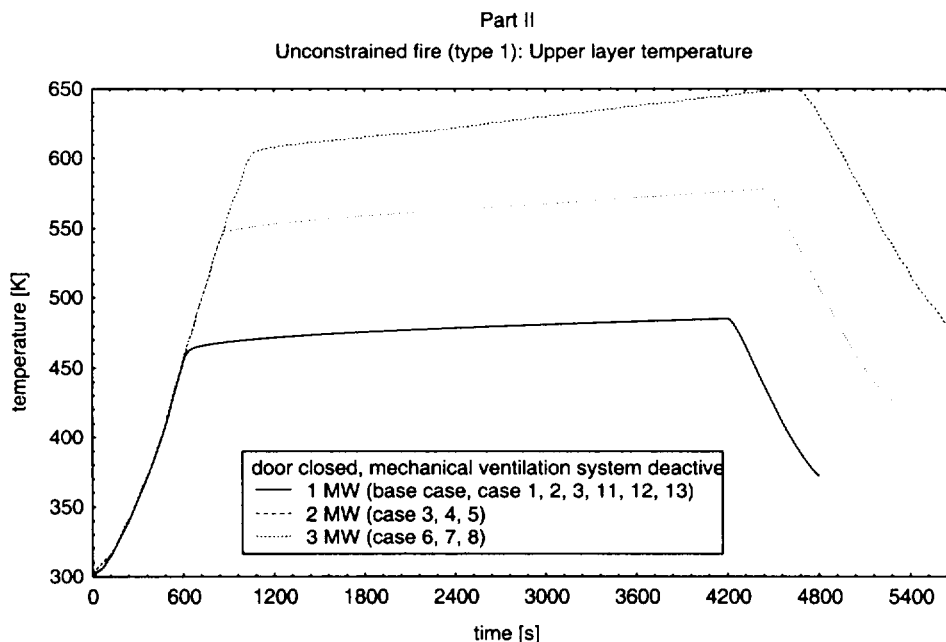


Figure 3.4 Effect of heat release rate: Upper layer temperature, unconstrained fire

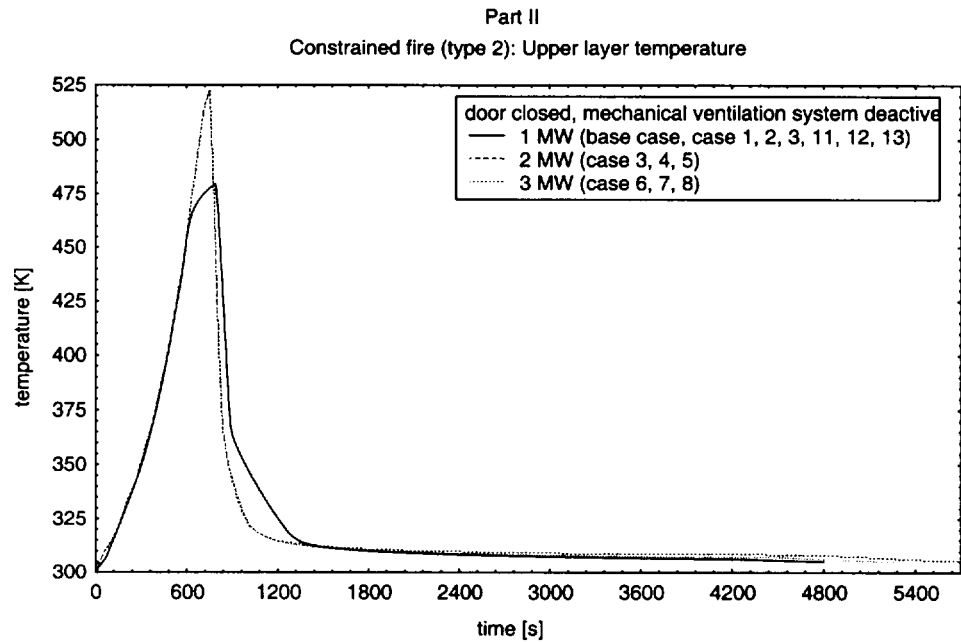


Figure 3.5 Effect of heat release rate: Upper layer temperature, constrained fire

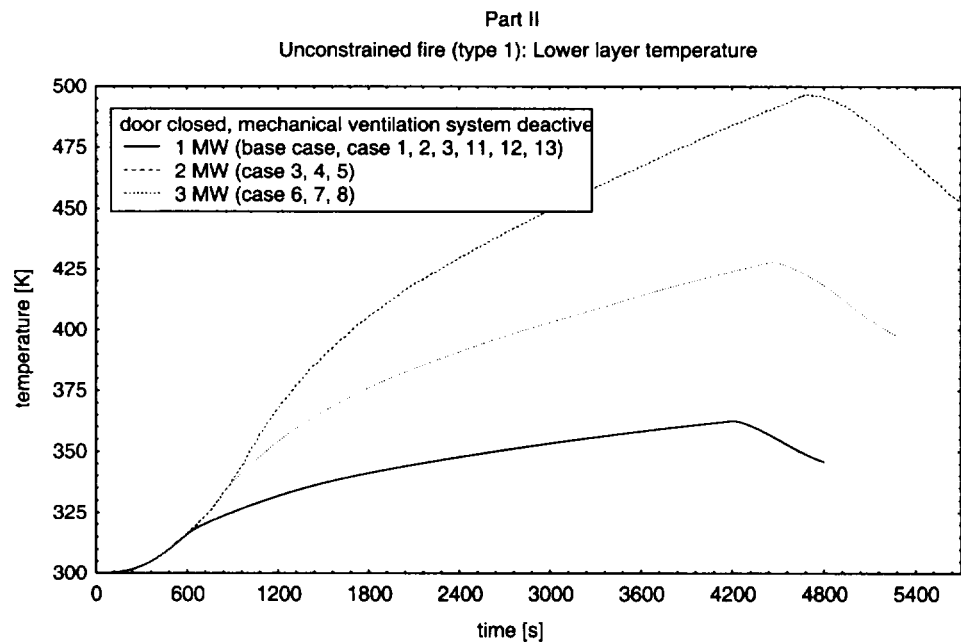


Figure 3.6 Effect of heat release rate: Lower layer temperature, unconstrained fire

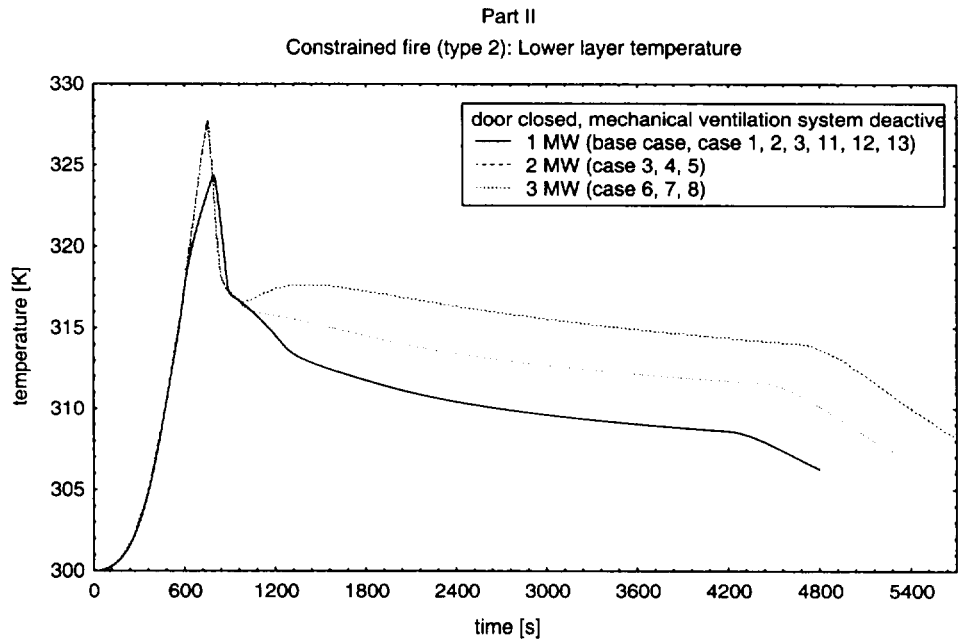


Figure 3.7 Effect of heat release rate: Lower layer temperature, constrained fire

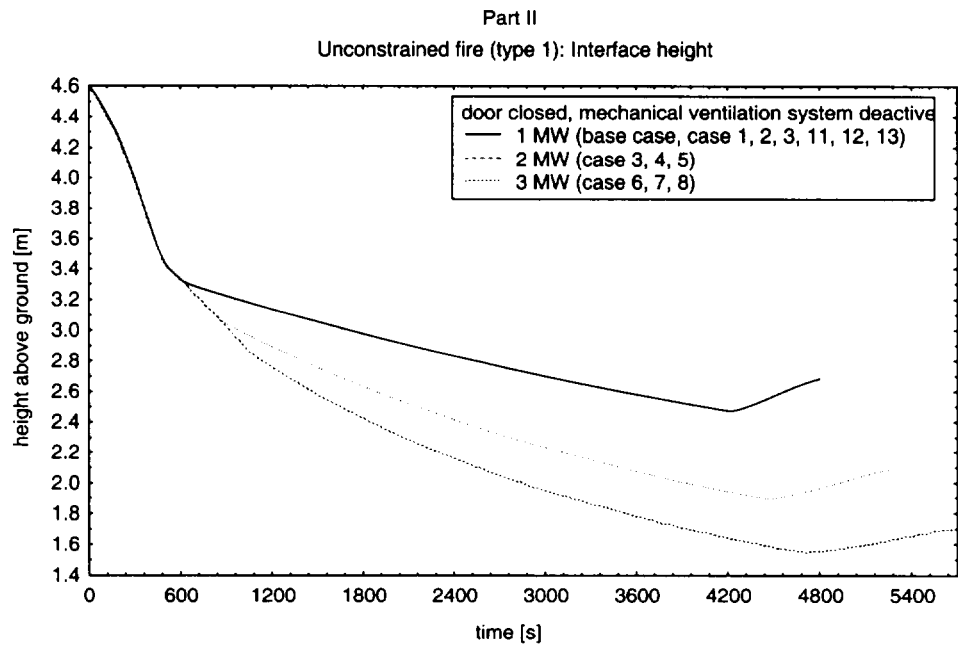


Figure 3.8 Effect of heat release rate: Interface height, unconstrained fire

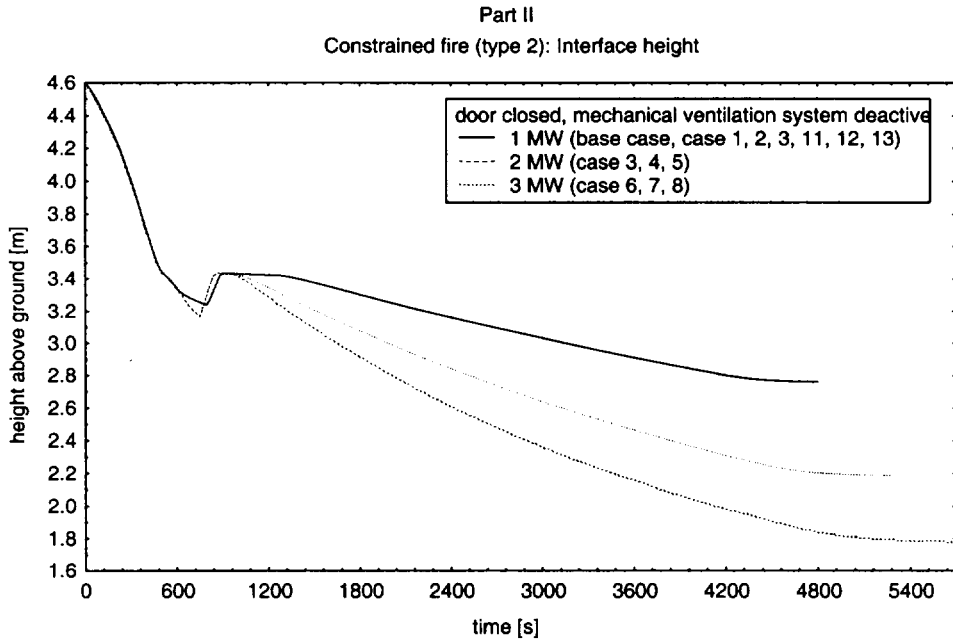


Figure 3.9 Effect of heat release rate: Interface height, constrained fire

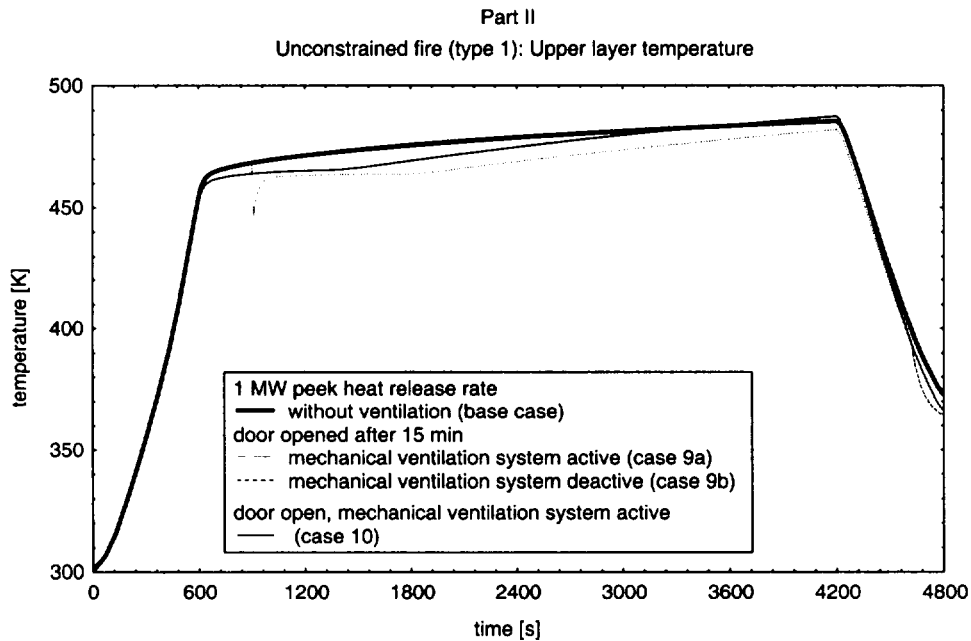


Figure 3.10 Effect of ventilation condition: Upper layer temperature, unconstrained fire

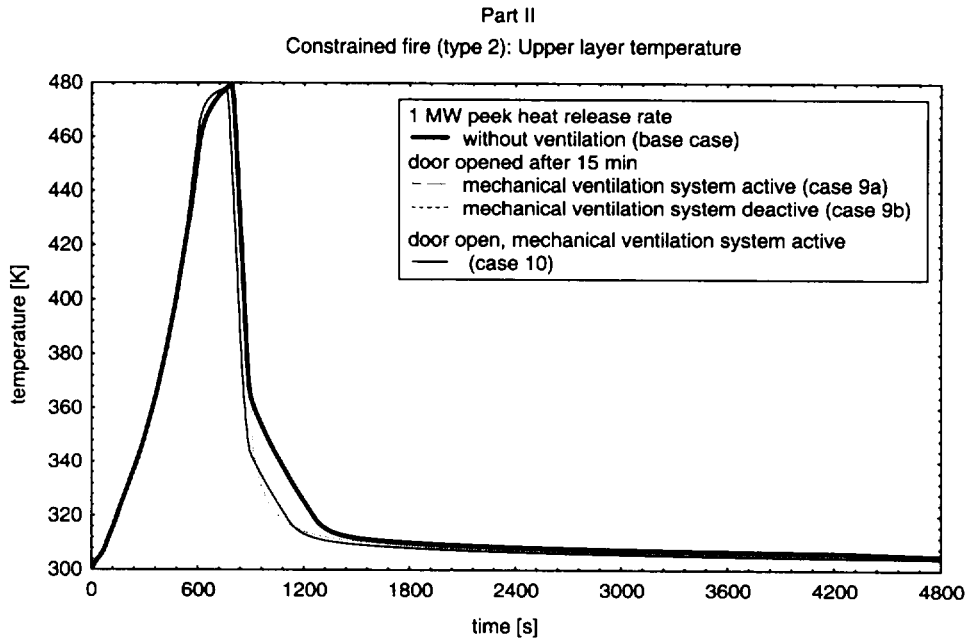


Figure 3.11 Effect of ventilation condition: Upper layer temperature, constrained fire

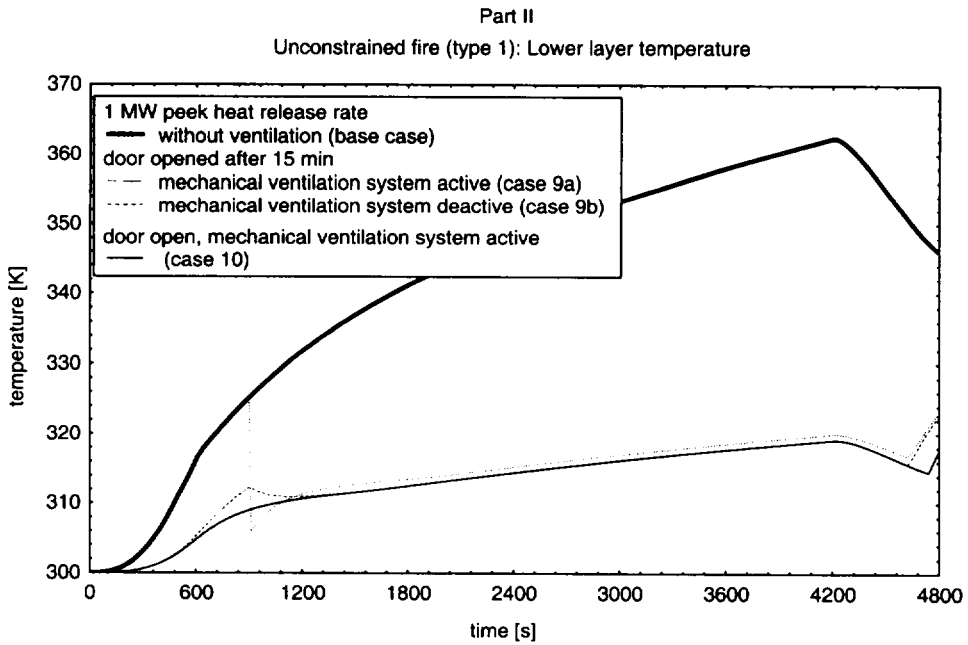


Figure 3.12 Effect of ventilation condition: Lower layer temperature, unconstrained fire

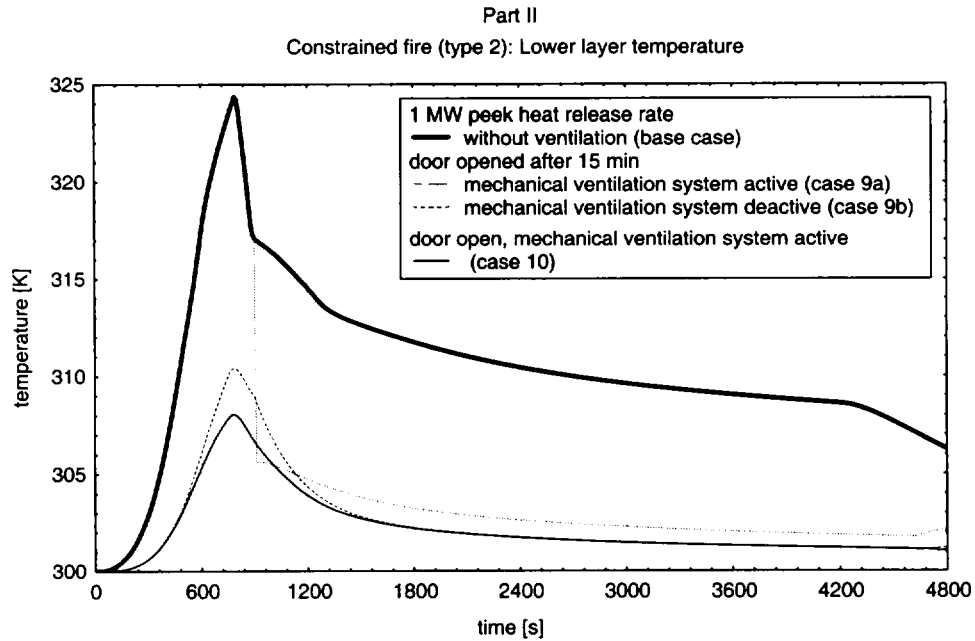


Figure 3.13 Effect of ventilation condition: Lower layer temperature, constrained fire

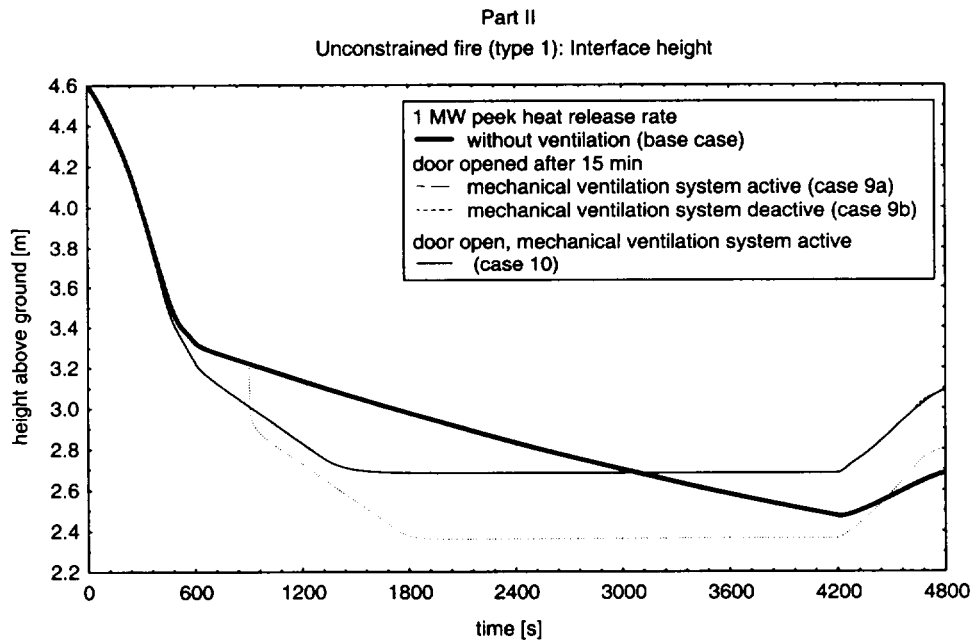


Figure 3.14 Effect of ventilation condition: Interface height, unconstrained fire

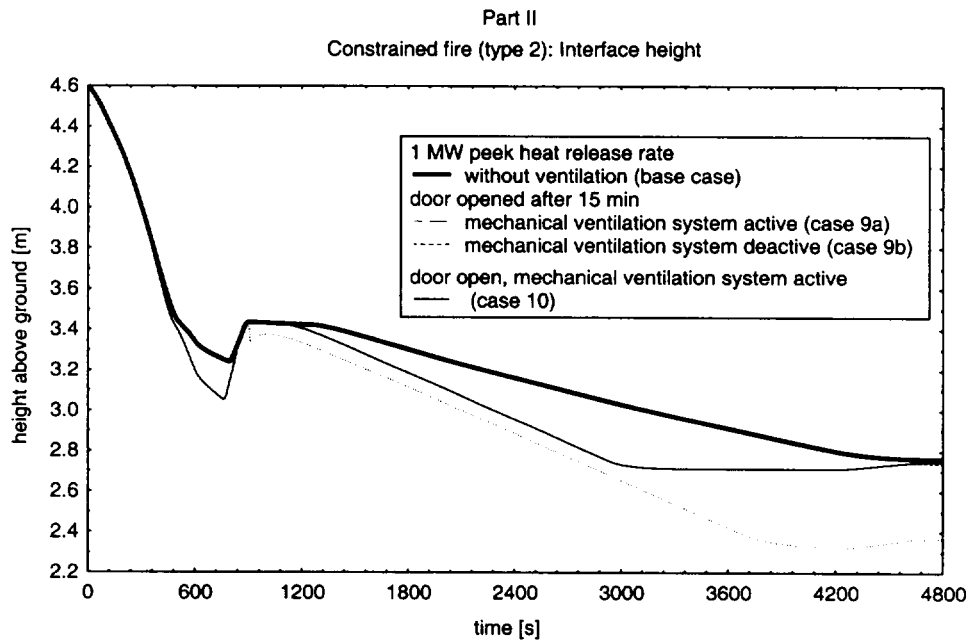


Figure 3.15 Effect of ventilation condition: Interface height, constrained fire

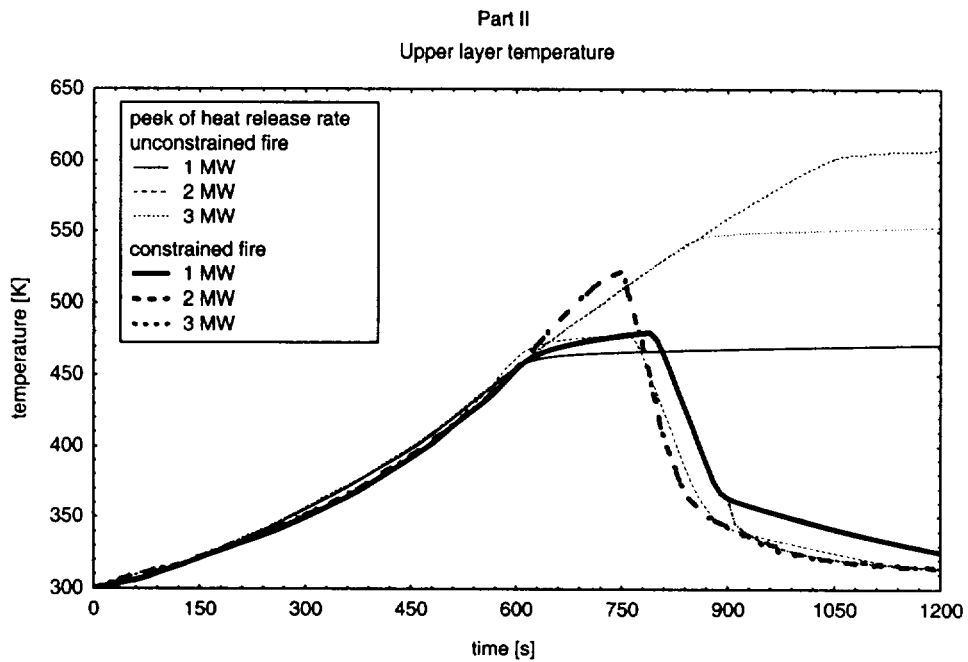


Figure 3.16 Effect of fire type: Upper layer temperature

Using the unconstrained fire algorithm (type 1), there is no restriction in the heat release rate. On the other hand, a maximum heat release rate of less than 1.5 MW is reached in case of using a constrained fire (type 2). In this case, a higher temperature of the upper layer is calculated until a lack of oxygen occurs. An increase of the heat release rate of course leads to an increase of the upper and lower layer temperatures and a decrease of the interface height.

Using the constrained fire algorithm (type 2), the oxygen contents of the upper and the lower layer are calculated. Neither the definition of the peak heat release rate nor the ventilation conditions seemed to have any remarkable influence on the oxygen content of the lower as well as of the upper layer (Figure 3.17).

It has been demonstrated that the vertical fire position has a strong effect on the course of the heat release rate. Using the same configurations and placing the fire on the floor level, the changes in the course of the upper layer oxygen content are calculated (Figure 3.18). The heat release rate decreases rapidly at that point of time at which the value of the oxygen content in the upper layer decreases to less than 1 %.

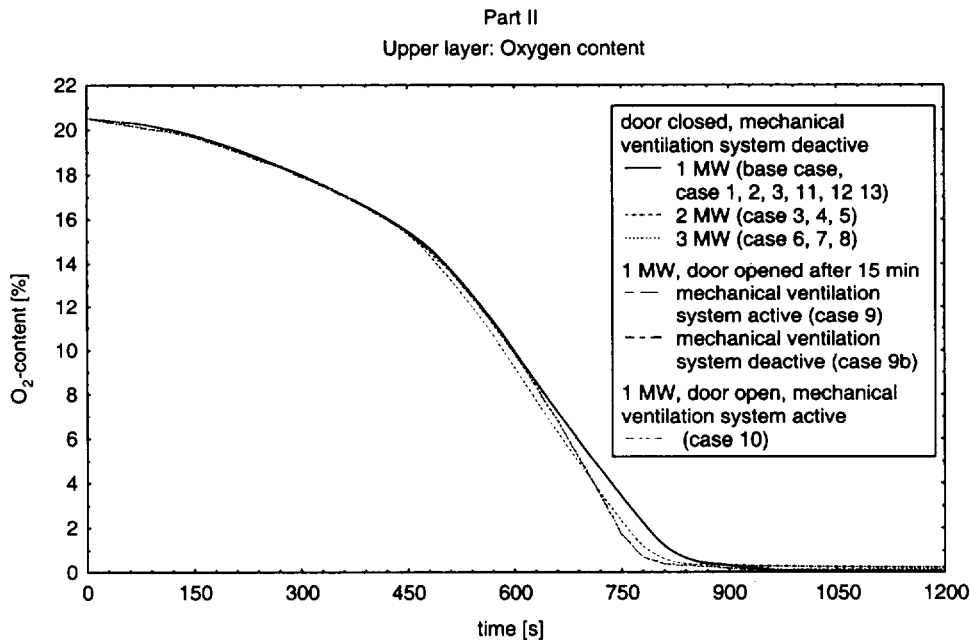


Figure 3.17 Effect of heat release rate and ventilation condition: Oxygen in the upper layer

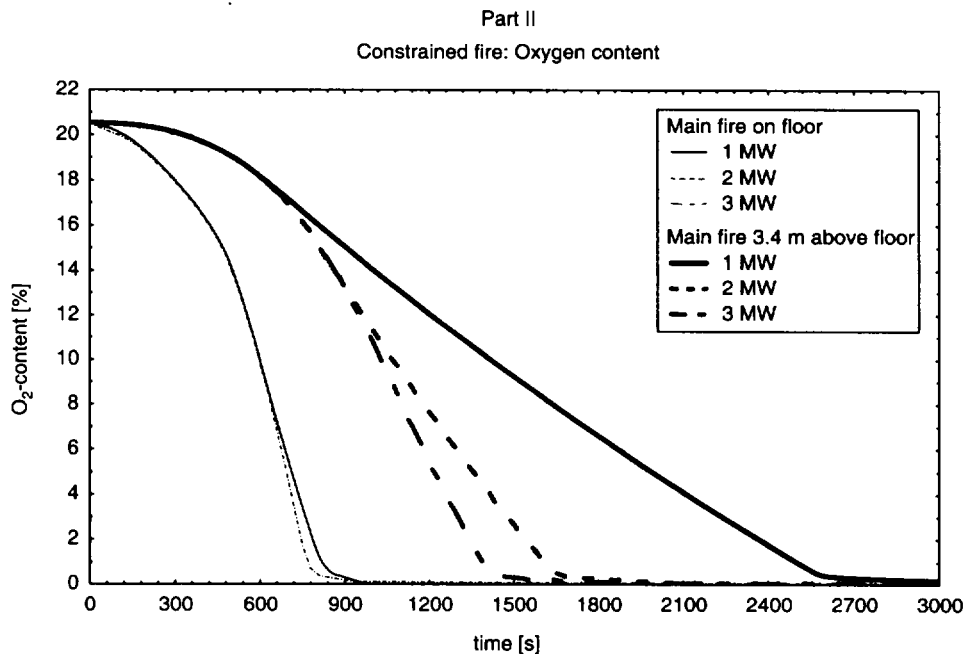


Figure 3.18 Effect of vertical fire position: Oxygen in the upper layer

If the mechanical ventilation system is active or the door is opened, only the upper layer temperature is affected. In case of using the unconstrained fire algorithm (type 1) it is slightly lower. The lower layer temperature is significantly lower in case of an additional ventilation and the interface height increases. In case of the door being opened and the mechanical ventilation system switched off (case 9b) the lower layer temperature reaches the lowest and the interface height reaches the highest level.

3.2.3 Mass flow rate of the mechanical ventilation system and through the opened door

Only in the cases 9 and 10 the door was assumed to be opened and the mechanical ventilation system was assumed to be used. As mentioned above, it was not possible to simulate deactivating the mechanical ventilation system while the calculation is still running, although it is possible to open or close a natural vent such as the door (using parameter CVENT).

The flow rates through the door and the vent (natural inflow) or the ducts of the mechanical ventilation system (forced outflow) are nearly independent of the fire algorithm until the fire is constrained by lack of oxygen. With very few exceptions, from this point of time the mass flow rates into the compartment and out of the compartment are higher if the constrained fire algorithm is used.

If there is no additional mechanical ventilation system (case 9b), nearly the same amount of gas flows through the door (after it has been opened) from outside into the lower layer as from the lower layer out of the compartment (Figure 3.19). As soon as the door has been opened while the mechanical ventilation system is running from the beginning (case 9a) the flow rates through the door become very soon equal to the flow rates calculated in case of the door being open all the time (case 10).

If there is no additional vent such as the door, a considerable amount of air flows into the lower layer through the vent (inflow) of the ventilation system (Figure 3.20). This mass flow stops and changes its direction (lower layer to outside) after the door has been opened (case 9a). Most of the gas, which is pumped through the ventilation system out of the compartment, is taken out of the lower layer (Figure 3.21). After 50 min simulation time a small amount of gas is also taken out of the upper layer (case 9a, case 10). The flow rates through the open door are not affected very much by the mechanical ventilation system. As soon as the door is opened the flow through the vent from outside into the lower layer stops.

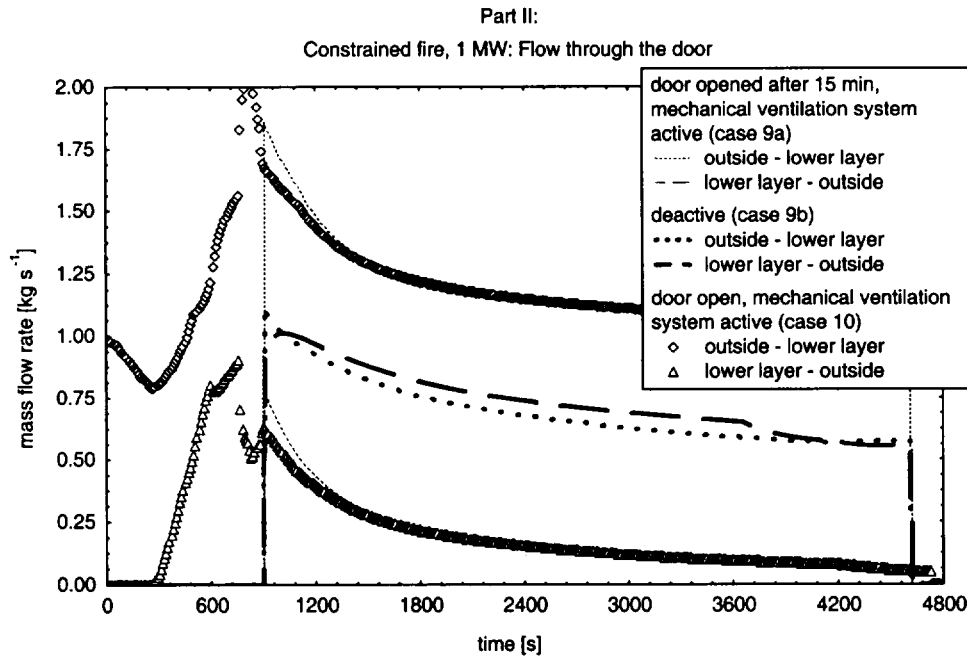


Figure 3.19 Effect of mechanical ventilation system: Mass flow rate through the door

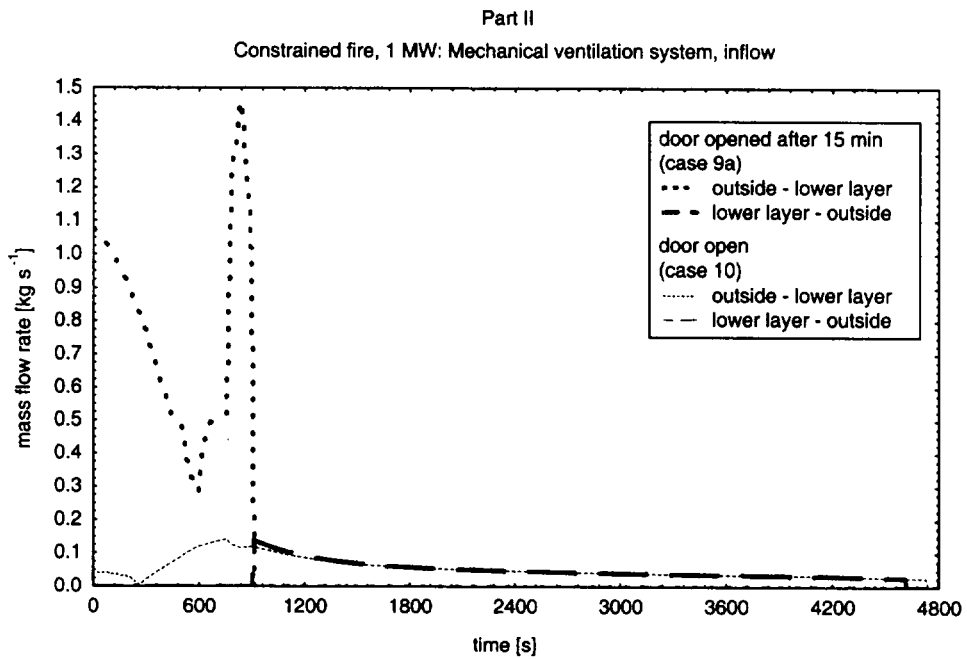


Figure 3.20 Effect of door opening: Mass flow rate through vent I (inflow)

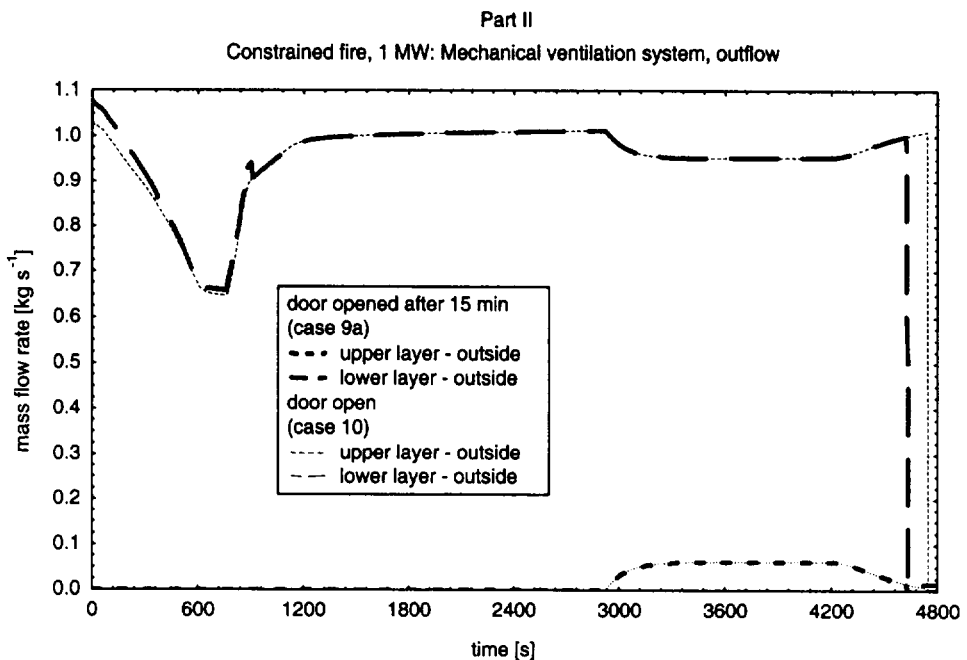


Figure 3.21 Effect of door opening: Mass flow rate through duct system (outflow)

3.2.4 Target surface temperature

Starting the calculations of Part II it was checked, whether the physical model of heating an object or target acts as in Part I, indicating that an object will always be assumed as being positioned in the center of a horizontal plane in the compartment. Obviously this happened, although the surface temperature is independent of the horizontal object position.

All other calculations of Part II were performed assuming that tray B (object / target) is placed in the center of the compartment (4.55 m, 7.6 m) and the main fire of tray A, C1, C2 (main fire) is moved in y-direction to get the distance D of 6.1 m (4.55 m, 1.5 m), 3.1 m (4.55 m, 4.5 m) or 4.6 m (4.55 m, 3.0 m). Prior to this calculations it had been demonstrated that it does not matter if the main fire is moved in x- or in y-direction.

The distance between the main fire of tray A, C1, C2 and the target tray B has only a minor effect on the surface temperature in case of an unconstrained fire (Figure 3.22). The differences between the maximum surface temperatures are small as well (Table 3.1). In case of a constrained fire the temperature does not increase very much (Figure 3.24). It does not make a difference whether the maximum heat release rate is 2 MW or 3 MW. This result is reasonable, because the calculations show that this level of the heat release rate is not reached. The distance between main fire and target has only small effects on the maximum surface temperature (Figure 3.26). The differences of the maximum surface temperatures are only 0.2 - 0.4 K.

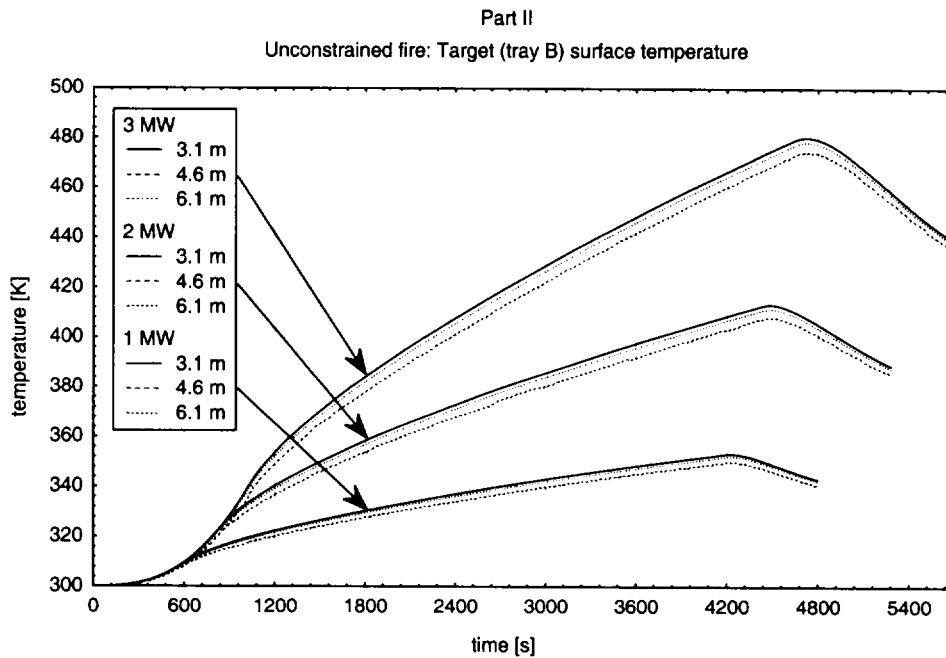


Figure 3.22 Effect of heat release rate and distance: Target (tray B) surface temperature

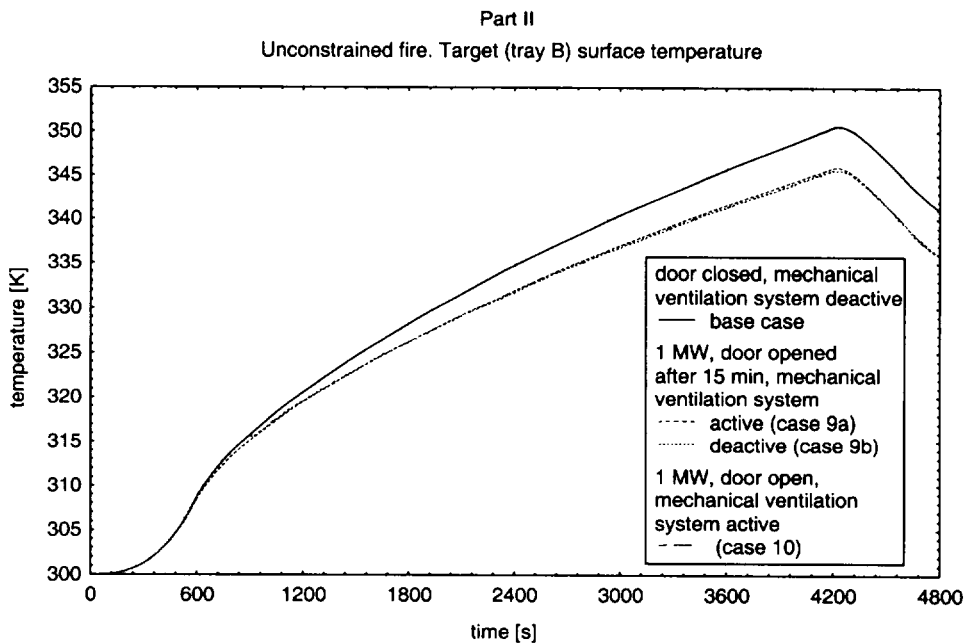


Figure 3.23 Effect of ventilation condition: Target (tray B) surface temperature

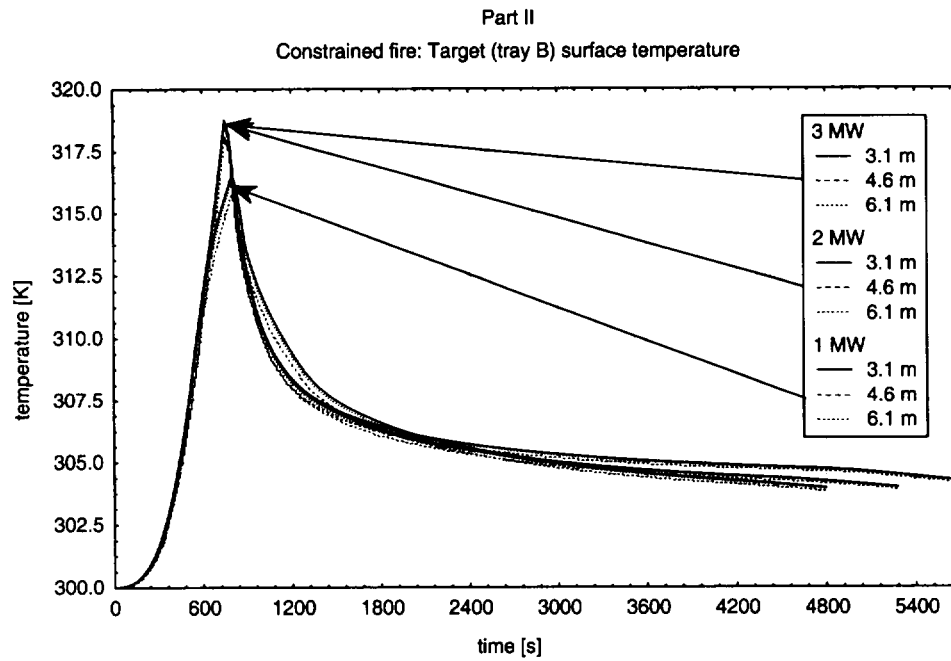


Figure 3.24 Effect of heat release rate and distance: Target (tray B) surface temperature

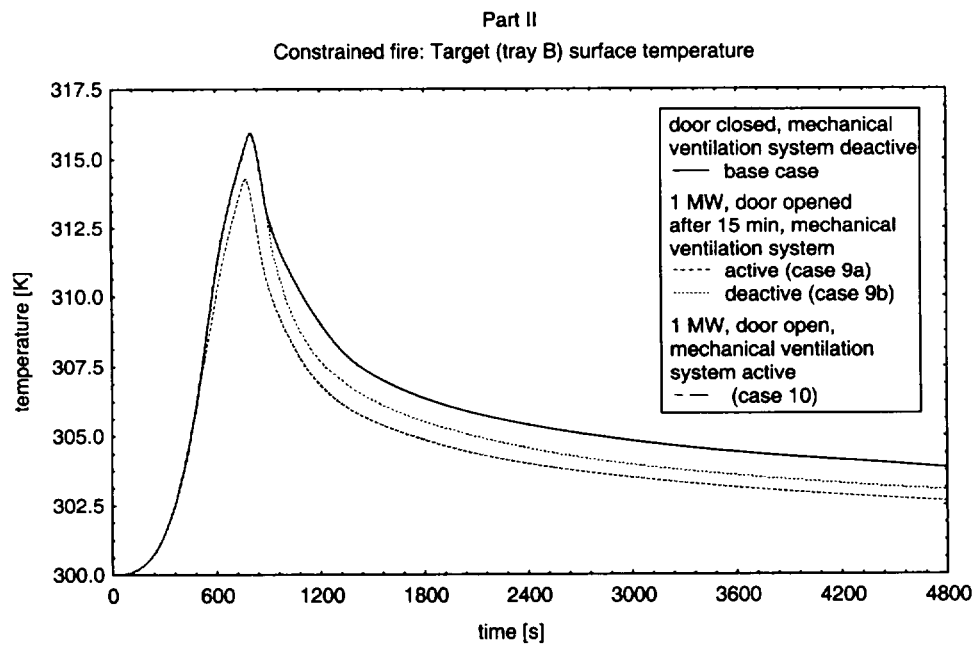


Figure 3.25 Effect of ventilation condition: Target (tray B) surface temperature

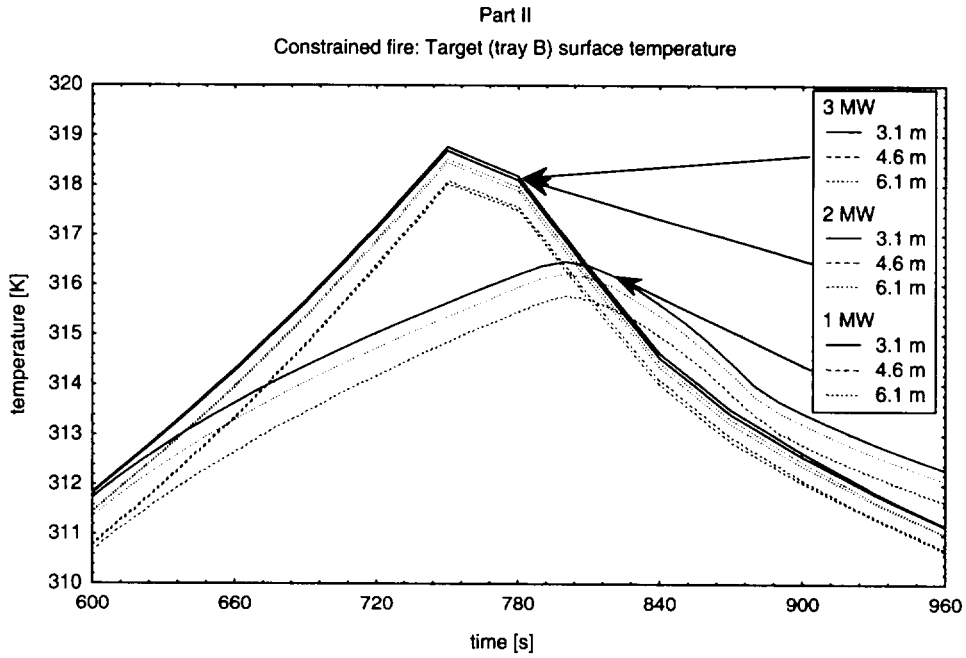


Figure 3.26 Effect of heat release rate and distance: Target (tray B) surface temperature

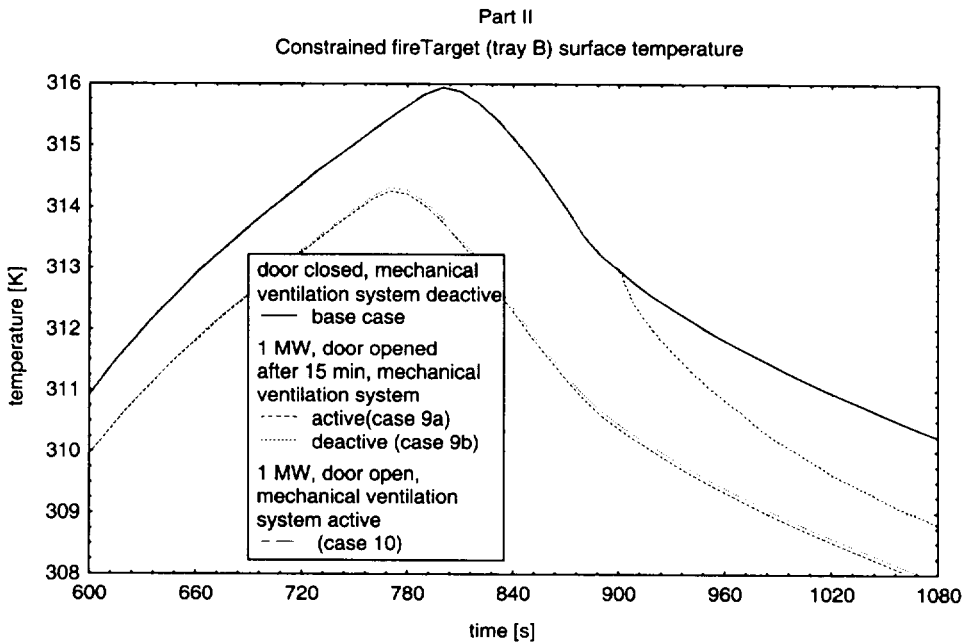


Figure 3.27 Effect of ventilation condition: Target (tray B) surface temperature

Table 3.1 Maximum target (tray B) surface temperature

Case	heat release rate	distance	maximum surface temperature	
			unconstrained fire	constrained fire
1	1 MW	3.1 m	353.33 K	316.22 K
2		4.6 m	352.17 K	316.47 K
base case		6.1 m	349.94 K	315.77 K
3	2 MW	3.1 m	413.33 K	318.70 K
4		4.6 m	411.56 K	318.45 K
5		6.1 m	408.08 K	318.02 K
6	3 MW	3.1 m	480.25 K	318.77 K
7		4.6 m	478.25 K	318.53 K
8		6.1 m	474.22 K	318.09 K

In case of an unconstrained fire the maximum target (tray B) surface temperature is approximately 6 K lower if the door is opened or the mechanical ventilation system is running (Figure 3.23). In case of a constrained fire, the maximum surface temperature is approximately 1.8 K lower if the mechanical ventilation system is running (Figure 3.27). In case that the mechanical ventilation system is not running and the door is opened after 15 min fire duration the temperature decreases a little faster (Figure 3.27).

4 CONCLUSIONS

The multi-room multi-zone model CFAST, version 4.0.1 has been applied to perform the calculations for the Benchmark Exercise # A “cable tray fires of redundant safety trains”. In Part I of this exercise the base case and five additional cases with varying distance between the trash bag as an ignition source and the tray A on the one hand and the ventilation conditions on the other are calculated. In addition, two fire algorithms are used. Defining a cable fire of tray A, C1, C2 the effects on cable tray B are studied in Part II of the Benchmark exercise. In this case, three different levels of heat release rate, different operation modes of the ventilation system, and door status as well as different cable diameters and tray elevations should be investigated.

The results calculated using the constrained fire algorithm seem to be more realistic. Nevertheless, there are some uncertainties. Particularly the upper layer temperature differs slightly in case

of a sufficient oxygen amount available comparing the two fire algorithms. The gas temperature and the layer thickness are calculated convincingly by CFAST. The mass flow rates through natural vents seem to be plausible. It is necessary to describe the main fire in more detail by defining the pyrolysis rate, the effective heat of combustion and the yields of combustion products, such as carbon dioxide, carbon monoxide and hydrochloride. It is obvious that the vertical position of the main fire has a strong influence on all results.

The computer code CFAST is not optimal for the Benchmark Exercise # 1 because the heat transfer to a target, as a main task of this exercise, is calculated by a very rough model. Due to this, no quantitative results can be produced. In addition, the forced ventilation model does not work in case of inflow. The composition of the incoming air seems to be wrong. Since it is not possible to define a time dependent fan power, switching the forced ventilation on or off cannot be simulated, but a mechanical ventilation system is a main tool to remove hot gases out of a fire compartment in a nuclear power plant.

Although CFAST does not seem to be appropriate for all of the questions of the given Benchmark Exercise, it is a very useful engineering tool for estimating fire and smoke transport in several other cases. The results of the CFAST calculations can be used to answer special questions such as heating of targets with more detailed models.

5 LITERATURE

- [1] Jones, W. W.; Forney, G. P.; Peacock, R. D.; Reneke, P. A.: A technical reference for CFAST: An engineering tool for estimating fire and smoke transport. NIST TN 1431, January 2000
- [2] Peacock, R. D.; Reneke, P. A.; Jones, W. W.; Bukowski, R. W.; Forney, G. P. A : User's guide for FAST: Engineering tools for estimating fire growth and smoke transport. NIST Special Publication 921 2000 Edition, January 2000
- [3] Peacock, R. D.; Forney, G. P.; Reneke, P. A.; Portier, R. M.; Jones, W. W.: CFAST, the consolidated model of fire and smoke transport. NIST Technical Note 1299, September 1995

- [4] Dey, M. K.: International Collaborative Project to Evaluate Fire Models for Nuclear Power Plant Applications: Benchmark Exercises #1, Cable tray fires of redundant safety trains, revised September 11, 2000

BIBLIOGRAPHIC DATA SHEET

(See instructions on the reverse)

1. REPORT NUMBER
(Assigned by NRC, Add Vol., Supp., Rev.,
and Addendum Numbers, if any.)

NUREG-1758

2. TITLE AND SUBTITLE

Evaluation of Fire Models for Nuclear Power Plant Applications: Cable Tray Fire s
International Panel Report

3. DATE REPORT PUBLISHED

MONTH	YEAR
June	2002

4. FIN OR GRANT NUMBER

N/A

5. AUTHOR(S)

Compiled by M. K. Dey

6. TYPE OF REPORT

Technical Report

7. PERIOD COVERED *(Inclusive Dates)*

N/A

8. PERFORMING ORGANIZATION - NAME AND ADDRESS *(If NRC, provide Division, Office or Region, U.S. Nuclear Regulatory Commission, and mailing address; if contractor, provide name and mailing address.)*

Division of Risk Analysis and Application (compiled by the NRC for an international expert panel)
Office of Nuclear Regulatory Research
U.S. Nuclear Regulatory Commission
Washington, DC 20555-0001

9. SPONSORING ORGANIZATION - NAME AND ADDRESS *(If NRC, type "Same as above"; if contractor, provide NRC Division, Office or Region, U.S. Nuclear Regulatory Commission, and mailing address.)*

Same as above

10. SUPPLEMENTARY NOTES

Report contains results of an international benchmark exercise for fire model verification and validation.

11. ABSTRACT *(200 words or less)*

This technical reference document was developed in the International Collaborative Project to Evaluate Fire Models for Nuclear Power Plant Applications. This volume reports on the results of the first task in the international collaborative project. The objective of the first task was to evaluate the capability of fire models to analyze cable tray fires of redundant safety systems in nuclear power plants. The evaluation of the capability of fire models to analyze these scenarios was conducted through an international benchmark exercise. Consideration of appropriate input parameters and assumptions, interpretation of the results, and determination of the adequacy of the physical sub-models established useful technical information regarding the capabilities and limitations of the fire models. The participants in the benchmark exercise determined that results indicate that the models provide a comprehensive treatment of most physical phenomena of interest in the scenarios analyzed. The predicted trends from the models were found to be similar and reasonable for their intended use. These fire models can provide useful results for nuclear power plant fire safety analysis for the types of scenarios analyzed.

12. KEY WORDS/DESCRIPTORS *(List words or phrases that will assist researchers in locating the report.)*

Nuclear safety
Fire models
Fire safety analysis
Validation and verification
Benchmarking
Cable tray fires
International review panel

13. AVAILABILITY STATEMENT

unlimited

14. SECURITY CLASSIFICATION

(This Page)

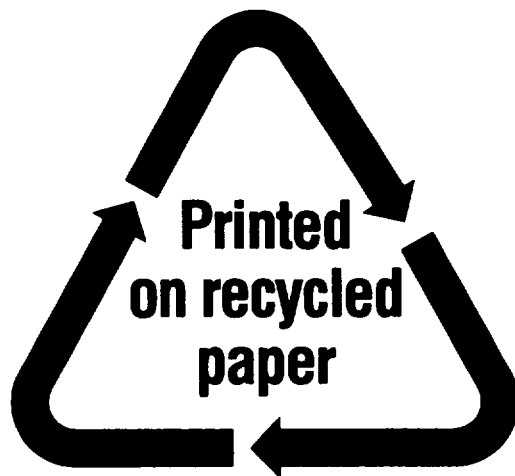
unclassified

(This Report)

unclassified

15. NUMBER OF PAGES

16. PRICE



Federal Recycling Program

ISBN 0-16-051153-4



9000

9 780160 511530

**UNITED STATES
NUCLEAR REGULATORY COMMISSION
WASHINGTON, DC 20555-0001**

**OFFICIAL BUSINESS
PENALTY FOR PRIVATE USE, \$300**